Since January 2020 Elsevier has created a COVID-19 resource centre with free information in English and Mandarin on the novel coronavirus COVID-19. The COVID-19 resource centre is hosted on Elsevier Connect, the company's public news and information website.

Chaos, Solitons and Fractals 139 (2020) 110281

Contents lists available at ScienceDirect

Chaos, Solitons and Fractals

Nonlinear Science, and Nonequilibrium and Complex Phenomena

journal homepage: www.elsevier.com/locate/chaos

Mathematical modeling, analysis and numerical simulation of the *COVID-19* transmission with mitigation of control strategies used in Cameroon

Seraphin Djaoue [a], Gabriel Guilsou Kolaye [a], Hamadjam Abboubakar [b], Ado Adamou Abba Ari [c,d,*], Irepran Damakoa [b]

[a] Department of Mathematics and Computer Science, University of Maroua, P.O. Box 814, Maroua, Cameroon
[b] LASE Lab, University of Ngaoundere, P.O. Box 455 Ngaoundere, Cameroon
[c] LaRI Lab, University of Maroua, P.O. Box 814 Maroua, Cameroon
[d] LI-PaRAD Lab, Université Paris Saclay, University of Versailles Saint-Quentin-en-Yvelines, 45 Avenue États-Unis Versailles cedex 78035, France

ARTICLE INFO

Article history:
Received 26 June 2020
Revised 27 August 2020
Accepted 8 September 2020
Available online 18 September 2020

Keywords:
Basic reproduction number
Extinction
Persistence
Backward
Quarantine
Testing
Masks

ABSTRACT

In this paper, we formulated a general model of *COVID-19* model transmission using biological features of the disease and control strategies based on the isolation of exposed people, confinement (lock-downs) of the human population, testing people living risks area, wearing of masks and respect of hygienic rules. We provide a theoretical study of the model. We derive the basic reproduction number $\mathcal{R}_0$ which determines the extinction and the persistence of the infection. It is shown that the model exhibits a backward bifurcation at $\mathcal{R}_0 = 1$. The sensitivity analysis of the model has been performed to determine the impact of related parameters on outbreak severity. It is observed that the asymptomatic infectious group of individuals may play a major role in the spreading of transmission. Moreover, various mitigation strategies are investigated using the proposed model. A numerical evaluation of control strategies has been performed. We found that isolation has a real impact on *COVID-19* transmission. When efforts are made through the tracing to isolate 80% of exposed people the disease disappears about 100 days. Although partial confinement does not eradicate the disease it is observed that, during partial confinement, when at least 10% of the partially confined population is totally confined, *COVID-19* spread stops after 150 days. The strategy of massif testing has also a real impact on the disease. In that model, we found that when more than 95% of moderate and symptomatic infected people are identified and isolated, the disease is also really controlled after 90 days. The wearing of masks and respecting hygiene rules are fundamental conditions to control the *COVID-19*.

1. Introduction

The *COVID-19*, also known as the coronavirus pandemic, is an ongoing pandemic of coronavirus disease 2019 (COVID-19), caused by severe acute respiratory syndrome coronavirus (SARS-CoV-2) [11]. The outbreak was first identified in Wuhan, China, in December 2019 [12,13]. The World Health Organization (WHO) declared the outbreak a Public Health Emergency of International Concern on 30th of January, and a pandemic on March 11 [14,15]. As of May 17, 2020, more than 463 million cases of *COVID-19* have been reported in more than 188 countries and territories, resulting in more than 311,000 deaths. More than 1.69 million people have recovered [16].

The virus is primarily spread between people during close contact, most often via small droplets produced by coughing, sneezing, and talking [17–19]. The droplets usually fall to the ground or onto surfaces rather than traveling through air over long distances [17]. Less commonly, people may become infected by touching a contaminated surface and then touching their face [17,18]. It is most contagious during the first three days after the onset of symptoms, although the spread is possible before symptoms appear, and from people who do not show symptoms [17,18].

Common symptoms include fever, cough, fatigue, shortness of breath, and loss of smell [17]. Complications may include pneumonia and acute respiratory distress syndrome [20] The time from exposure to onset of symptoms is typically around five days, but may range from two to fourteen days [21,22]. Actually, there is no

* Corresponding author at: LI-PaRAD Lab, Université Paris Saclay, University of Versailles Saint-Quentin-en-Yvelines, 45 Avenue États-Unis, 78035 Versailles cedex, France.
E-mail address: adoadamou.abbaari@gmail.com (A.A. Abba Ari).

https://doi.org/10.1016/j.chaos.2020.110281
0960-0779/

known vaccine or specific antiviral treatment [17]. Primary treatment is symptomatic and supportive therapy [23].

Furthermore, recommended preventive measures include hand washing, covering one's mouth when coughing, maintaining distance from other people, wearing a face mask in public settings, and monitoring and self-isolation for people who suspect they are infected [17]. Authorities worldwide have responded by implementing travel restrictions, lock-downs, workplace hazard controls, and facility closures. Many places have also worked to increase testing capacity and trace contacts of infected persons.

Moreover, the pandemic has caused severe global economic disruption [24], including the largest global recession since the Great Depression [25]. It has led to the postponement or cancellation of sporting, religious, political, and cultural events [26], widespread supply shortages exacerbated by panic buying [27], and decreased emissions of pollutants and greenhouse gases [28]. Schools, universities, and colleges have been closed either on a nationwide or local basis in 186 countries, affecting approximately 98.5 percent of the world's student population [29].

Besides, the *COVID-19* pandemic was confirmed to have spread to Africa on February 14, 2020. The first confirmed case was in Egypt [30,31], and the first confirmed case in sub-Saharan Africa was in Nigeria [32]. Most of the identified imported cases have arrived from Europe and the United States rather than from China [33]. Most of the reported cases are from four countries: South Africa, Morocco, Egypt, and Algeria, but it is believed that there is widespread under-reporting in other African countries with less developed healthcare systems [34].

Thereby, the *COVID-19* pandemic was confirmed to have spread to Cameroon, Central Africa on March 6, with its first confirmed case [35]. The infected person is a French national who arrived in the capital Yaoundé on February 24, [36]. On May 5, Cameroon had 2104 confirmed cases and 64 deaths [37] vs. 7392 confirmed cases on June 6, with 205 deaths [54]. On March 18, Cameroonian Prime Minister Joseph Dion Ngute closed its land, air, and sea borders [38]. Then, on March 30, Cameroon's Minister of Health announced the imminent launch of a coronavirus test campaign in the city of Douala. Dedicated teams will go door-to-door in the economic capital from April 2, to 6, says the minister [39]. On April 10, the government took 7 additional measures to stop the spread of *COVID-19* in Cameroon. These measures take effect from Monday, April 13, 2020 [40]: wearing a mask in all areas open to the public; local establishment of specialized *COVID-19* treatment centers in all regional capitals; intensification of the screening campaign with the collaboration of the Center Pasteur; intensification of the awareness campaign in urban and rural areas in both official languages; Continuation of activities essential to the economy in strict compliance with the Prime Minister directives of March 17, 2020; and sanction. On Tuesday, May 5, the Minister of Health announced the provision to healthcare personnel of 50,000 coveralls, 320,000 surgical masks, 220 backpack sprayers, 10,000 pairs of overshoes [42].

Cameroon government choices control strategies based specially on; isolation of exposed or infected people, partial confinement, testing people of risk areas, and mandatory wearing of masks. Until now, no one mathematical model has been suggested modeling the real situation of *COVID-19* propagation in Cameroon, to evaluate and to analyze various strategies used by the government to avoid hatching of *COVID-19* disease in Cameroon. The present work is strongly motivated to suggest a general framework of *COVID-19* simulation integrating real specificities of Cameroon and providing numerical evaluation and comparison of control strategies used by Cameroonian authorities. In literature, numerous general mathematical models have been published to analyze *COVID-19* outbreaks in an effort to better understand the complex disease transmission [45–53,61–63]. But to our knowledge, few of these have specifically taken control actions into consideration [61].

In this paper, we formulated a mathematical model for the *COVID-19* disease, which incorporates some key epidemiological and biological features of the disease such as variation infection form, control strategies taking account on some specificities of the Cameroon population. The novelty of our model is based on his adequacy to the real situation of Cameroon. Since it is so difficult to confine totally population, government make many efforts to identify and isolate exposed peoples. From the 14th March 2020 Cameroonian government take some decisions to put the population in a context of partial confinement and total confinement for students. For instance, schools and universities are closed. Many administrations reduced their daily personal or/and the daily duration of their activities. That's why it is important to consider the class of susceptible people who consider and apply these measures of partial confinement and total confinement. Another particularity of the model concerns variation of infection form which is very important on epidemiological view. The model suggested was deeply analyzed and numerical simulations have been performed to supported theoretical studies and to illustrate the effectiveness of each control strategy integrated. The sensitivity analysis of the model is carried out to identify the most influential parameters on the model output variables related to infected classes, which is the most robust estimations that are required.

The rest of the paper is organized as follows. After the formulation of the model in Section 2, we present its quantitative and qualitative analysis in Section 3. Numerical simulations are provided in Section 4. The last section is devoted to concluding remarks on how our work fits in the literature.

2. Model formulation

The proposed model classifies the human population according to the disease status and to the level exposition to the disease, namely: susceptible individuals S, quarantined individual Q, partially confined individuals C_p, totally confined individuals C_t, individuals in latency phase L, infected individuals with asymptomatic form I_a, infected individuals with benign (moderated) form I_b, infected individuals with serious form I_s, quarantined infected individuals I_q and recovered individuals R. Thus, the total human population at time t denoted by $N(t)$ is given by Eq. (1).

$$N(t) = S(t) + Q(t) + C_p(t) + C_t(t) + L(t) + I_a(t) + I_b(t) + I_s(t) + I_q(t) + R(t). \quad (1)$$

The population of *coronavirus* is denoted by V. The susceptible individuals are recruited through birth and immigration at a constant rate of Λ. The disease can be transmitted directly through oral or nasal ingestion of droplets generated when an infected person coughs or sneezes, or indirectly through oral or nasal ingestion of droplets of saliva or discharge the nose of infected individuals left in environment [17–19]. Thus, the infection is regulated by the exposure with infected individuals at rates $\beta_h(I_a + I_b + I_s)/N$ where β_h is the human-to-human per capita contact rate per unit time. Also, infection is regulated by the exposure with a free virus in nature at rates β_v per unit of time through the logistic dose-response $V/(V + K)$ where K is a concentration of free virus that yields 50% of chance for a susceptible individual to catch *COVID-19*. Thus, the force of infection is given in Eq. (2).

$$\lambda_s = (1 - \pi)\left[\beta_h \frac{I_a + I_b + I_s}{N} + \beta_v \frac{V}{V + K}\right] \quad (2)$$

where π is the proportion of infectious contact identified by public health workers.

In Cameroon, individuals partially confined are supposed able only to go work and market (for catering) but should avoid being where there are many people (more than 50) like mosques,

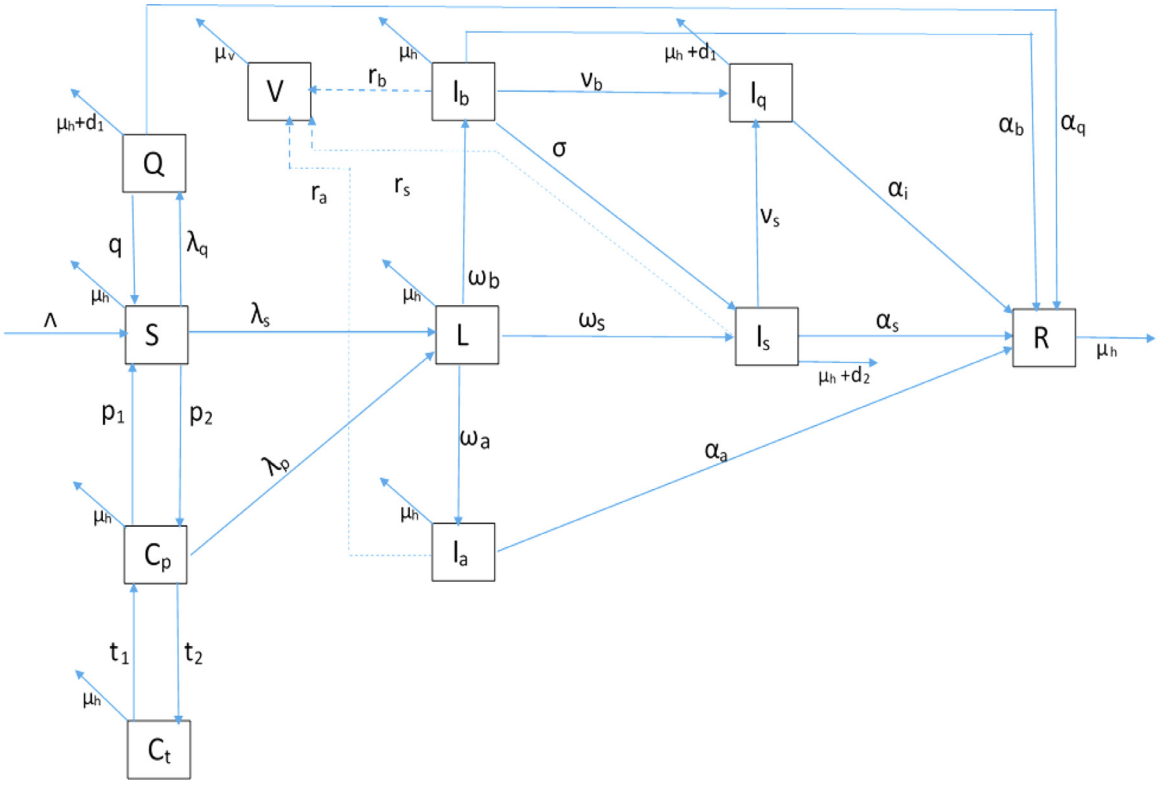

Fig. 1. Flow chart of the transmission dynamics of the *COVID-19* model.

churches, beer-houses, snack bars, etc. [1,40,41]. The people partially confined are exposed to the disease through the force of infection $\lambda_p = \epsilon\lambda_s$ where ϵ is the modification parameter which takes into account the fact that people partially confined are less exposed than the susceptible individuals. The susceptible individuals apply partial confinement rules at the rate p_2 and return to classical habits at rate p_1. When the situation becomes dramatic, the partial confinement could tends to the total confinement at the rate of t_2 and return to partial confinement t_1.

Susceptible individuals who have been known exposed with infected individuals or individuals in latency phases should be quarantined to observe their disease status and anticipate their treatment if it is necessary. This strategy control strategy reduces the expansion of the disease and its lethality. Thus, the force of infection, in this case, is given by Eq. (3).

$$\lambda_q = \pi\beta_h \frac{\kappa L + I_a + I_b + I_s}{N} \tag{3}$$

where the modification parameter $0 \leq \kappa \leq 1$ accounts for the assumed reduction in transmissibility of latent individuals relative to infectious individuals. During isolation, if they have a negative test they will return in susceptible class. But if they have a positive test, they will be treated. They can heal at the rate of α_q or die at the rate of d_1.

After the latency phase, most people with the *COVID-19* will experience an asymptomatic form of infection at the rate of ω_a and others will experience moderate respiratory illness at the rate of ω_b. In the two cases, they will recover without requiring special treatment α_a and α_b respectively. The older people and those with underlying medical problems like cardiovascular disease, diabetes, chronic respiratory disease and cancer are more likely to develop a serious illness at the rate of ω_s. Those who experience moderate respiratory illness may, at rate σ, develop serious illness in case of superinfection or coinfection with malaria, influenza, or typhoid which are endemic diseases in Cameroon. The infected individuals who are not quarantined (I_a, I_b and I_s) broadcast the virus in the environment at constant rates r_a, r_b and r_s respectively. The pathogens are assumed to decay at a rate of μ_v. Through a test campaign launched by the Cameroonian government, most of those experiences moderate and serious can be tested and quarantined at the rate of ν_b and ν_s respectively. The infected individuals with serious form I_s and the quarantined infected individuals I_q can recover from the disease at constant rates α_s and α_i respectively. The infected individual who experiences a serious form of disease I_s can die because of disease at a constant rate of d_2. Infected individuals quarantined (I_q and Q) could die due to the disease at the rate d_1 (which is supposed be less than d_2). The human population is submitted to the natural mortality of μ_h.

The structure of the model is shown in Fig. 1. The dashed arrow indicates contamination of the environment by infected humans.

The dynamics of the disease can be described by the following system of non-linear differential equations:

$$\begin{cases} \dot{S} = \Lambda + qQ + p_1C_p - (\lambda_q + \lambda_s + \mu_h + p_2)S, \\ \dot{C}_p = p_2S + t_1C_t - (\lambda_p + p_1 + t_2 + \mu_h)C_p, \\ \dot{C}_t = t_2C_p - (t_1 + \mu_h)C_t, \\ \dot{Q} = \lambda_qS - (q + \alpha_q + \mu_h + d_1)Q, \\ \dot{L} = \lambda_sS + \lambda_pC_p - (\omega_a + \omega_b + \omega_s + \mu_h)L, \\ \dot{I}_a = \omega_aL - (\alpha_a + \mu_h)I_a \\ \dot{I}_b = \omega_bL - (\nu_b + \sigma + \alpha_b + \mu_h)I_b \\ \dot{I}_q = \nu_bI_b + \nu_sI_s - (\alpha_i + \mu_h + d_1)I_q \\ \dot{I}_s = \omega_sL + \sigma I_b - (\nu_s + \alpha_s + \mu_h + d_2)I_s \\ \dot{R} = \alpha_aI_a + \alpha_bI_b + \alpha_sI_s + \alpha_iI_q + \alpha_qQ - \mu_hR \\ \dot{V} = r_aI_a + r_bI_b + r_sI_s - \mu_vV \end{cases} \tag{4}$$

We set $k_1 = \mu_h + p_2$, $k_2 = p_1 + t_2 + \mu_h$, $k_3 = t_1 + \mu_h$, $k_4 = q + \alpha_q + \mu_h + d_1$, $k_5 = \omega_a + \omega_b + \omega_s + \mu_h$, $k_6 = \alpha_a + \mu_h$, $k_7 = \nu_b + \sigma + \alpha_b + \mu_h$, $k_8 = \alpha_i + \mu_h + d_1$ and $k_9 = \nu_s + \alpha_s + \mu_h + d_2$.

The parameter values of system (4) used for numerical simulations are given in Table 1.

Table 1
Numerical values for the parameters of model system (4).

Definition	Parameter	Value	Source
Recruitment rate	Λ	10 day^{-1}	Assumed
Natural mortality rate of humans	μ_h	0.0104 day^{-1}	[2]
Exposure rate to infected individual	β_h	0.18 person^{-1} day^{-1}	[5]
Exposure rate to environmental virus	β_v	0.18 day^{-1}	[5]
Exiting rate of quarantine of exposed individual	q	0.14 day^{-1}	Assumed
Partial confinement rate of Susceptible individual	p_2	0.04 day^{-1}	[6]
Total confinement rate of partial confined individual	t_2	0.001 day^{-1}	Assumed
Exiting rate of partial confinement	p_1	0.01 day^{-1}	[7]
Exiting rate of total confinement	t_1	0.03 day^{-1}	Assumed
COVID-19 induced mortality with treatment	d_1	0.06 day^{-1}	[4]
COVID-19 induced mortality without treatment	d_2	0.1 day^{-1}	[4]
Half saturation constant	K	10^6	Assumed
Proportion of asymptomatic infected individual	ω_a	0.1	[3]
Proportion of benign infected individual	ω_b	0.8	[3]
Proportion of symptomatic infected individual	ω_s	0.1	[3]
Pathogen shed rate of asymptomatic infected individual	r_a	0.01	Assumed
Pathogen shed rate of benign infected individual	r_b	0.05	Assumed
Pathogen shed rate of symptomatic infected individual	r_s	0.1	Assumed
Decay rate of virus	μ_v	0.1	Assumed
Rate at which benign infection become symptomatic	σ	0.14	[4]
Rate at which benign infected are quarantined	ν_b	0.1	Assumed
Rate at which symptomatic infected are quarantined	ν_s	0.14	Assumed
Recovery rate of asymptomatic infected individual	α_a	0.07	[3]
Recovery rate of benign infected individual	α_b	0.03	[4]
Recovery rate of symptomatic infected individual	α_s	0.03	[4]
Recovery rate of quarantined infected individual	α_i	0.07	[3]
Recovery rate of exposed individual	α_q	0.07	[3]
Proportion of infectious contact identified	π	0.1	Assumed
Modification parameter	ϵ	0.5	Assumed
Modification parameter	κ	0.5	Assumed

3. Mathematical analysis

3.1. Basic properties

3.1.1. Positivity of solutions

We investigate the asymptotic behavior of orbits starting in the nonnegative cone $\mathbb{R}^{11}_+$. Obviously, model (4) which is a C^∞ differential system, admits a unique maximal solution for any associated Cauchy problem.

Theorem 3.1. *Let* $(t_0 = 0, X_0 = (S(0), C_t(0), C_p(0), Q(0), L(0), I_a(0), I_b(0), I_q(0), I_s(0), R(0), V(0))) \in \mathbb{R} \times \mathbb{R}^{11}_+$ *and for* $T \in]0, +\infty]$, $([0, T[, X = (S(t), C_t(t), C_p(t), Q(t), L(t), I_a(t), I_b(t), I_q(t), I_s(t), R(t), V(t)))$ *the maximal solution of the Cauchy problem associated to model* (4). *Then,* $\forall t \in [0; T[, X(t) \in \mathbb{R}^{11}_+$.

Proof: Let

$$\Delta = \Big\{\tilde{t} \in [0; T[\mid S(t) > 0,\ C_t(t) > 0,\ C_p(t) > 0,\ Q(t) > 0,\ L(t) > 0,\ I_a(t) > 0, I_b(t) > 0,\ I_q(t) > 0,\ I_s(t) > 0,\ R(t) > 0,\ V(t) > 0,\ \forall t \in]0, \tilde{t}[\Big\}.$$

By continuity of function S, C_t, C_p, Q, L, I_a, I_b, I_q, I_s, R and V one can see that $\Delta \neq \emptyset$. Let $\tilde{T} = \sup \Delta$. Now, we are going to show that $\tilde{T} = T$. Suppose $\tilde{T} < T$, then one has that S, C_t, C_p, Q, L, I_a, I_b, I_q, I_s, R and V are non negative on $[0; \tilde{T}[$. At $\tilde{T}$, at least one of the following conditions is satisfied $S(\tilde{T}) = 0$, $C_t(\tilde{T}) = 0$, $C_p(\tilde{T}) = 0$, $Q(\tilde{T}) = 0$, $L(\tilde{T}) = 0$, $I_a(\tilde{T}) = 0$, $I_b(\tilde{T}) = 0$, $I_q(\tilde{T}) = 0$, $I_s(\tilde{T}) = 0$, $R(\tilde{T}) = 0$ and $V(\tilde{T}) = 0$. Suppose $S(\tilde{T}) = 0$, then from the first equation of model (4), one has

$$\frac{d}{dt}\left(Se^{\int_0^t (\lambda_q(r)+\lambda_s(r)+p_2+\mu_h)dr}\right) = (\Lambda + qQ + p_1C_p)e^{\int_0^t (\lambda_q(r)+\lambda_s(r)+p_2+\mu_h)dr}. \tag{5}$$

Integrating Eq. (5) from 0 to $\tilde{T}$ yields

$$S(\tilde{T}) = e^{-\int_0^{\tilde{T}} (\lambda_q(r)+\lambda_s(r)+p_2+\mu_h)dr}\left(S(0) + \int_0^{\tilde{T}} \left(e^{\int_0^t (\lambda_q(r)+\lambda_s(r)+p_2+\mu_h)dr}\right).$$
$$(\Lambda + qQ(t) + p_1C_p(t)dt) > 0.$$

Similarly, one can show that $C_t(\tilde{T}) > 0$, $C_p(\tilde{T}) > 0$, $Q(\tilde{T}) > 0$, $L(\tilde{T}) > 0$, $I_a(\tilde{T}) > 0$, $I_b(\tilde{T}) > 0$, $I_q(\tilde{T}) > 0$, $I_s(\tilde{T}) > 0$, $R(\tilde{T}) > 0$ and $V(\tilde{T}) > 0$. This is a contradiction. Then, $\tilde{T} = T$ and consequently the maximal solution $(S(t), C_t(t), C_p(t), Q(t), L(t), I_a(t), I_b(t), I_q(t), I_s(t), R(t), V(t)))^T$ of the Cauchy problem associated to model (4) is positive. This achieves the proof.

□

3.1.2. Boundedness of solutions

We first split the model (4) into two parts, the human population, and the virus population. Then, using a model (4), the dynamics of the total human population satisfy

$$\dot{N} = \Lambda - \mu_h N - d_1(Q + I_q) - d_2 I_s \leq \Lambda - \mu_h N. \tag{6}$$

Integrating the above differential inequality yields

$$0 \leq N(t) \leq \frac{\Lambda}{\mu_h} + \left(N(0) - \frac{\Lambda}{\mu_h}\right)e^{-\mu_h t}, \qquad \forall t \geq 0,$$

where $N(0)$ is the initial value of $N(t)$. It implies that $0 \leq N(t) \leq \frac{\Lambda}{\mu_h}$ for all $t \geq 0$ if $N(0) \leq \frac{\Lambda}{\mu_h}$.

Now, suppose that $N(0) \leq \frac{\Lambda}{\mu_h}$, using the fact that $I_a(t) + I_b(t) + I_s(t) \leq \Lambda/\mu_h$, the dynamics of virus satisfies

$$\dot{V} \leq \frac{r\Lambda}{\mu_h} - \mu_v V, \tag{7}$$

where $r = \max(r_a, r_b, r_s)$. Integrating Eq. (7) gives

$$0 \leq V(t) \leq \frac{r\Lambda}{\mu_v\mu_h} + \left(V(0) - \frac{r\Lambda}{\mu_v\mu_h}\right)e^{-\mu_v t}, \qquad \forall t \geq 0,$$

where $V(0)$ represents the initial value of $V(t)$. It implies that $0 \leq V(t) \leq \frac{r\Lambda}{\mu_v\mu_h}$ for all $t \geq 0$ if $V(0) \leq \frac{r\Lambda}{\mu_v\mu_h}$.

It then follows that

$$N(t)+V(t) \leq \max\left(N(0)+V(0), \frac{\Lambda}{\mu_h}\left(1+\frac{r}{\mu_v}\right)\right), \qquad \forall t \geq 0. \tag{8}$$

Thus, the region:

$$\Omega = \left\{(S, C_t, C_p, Q, L, I_a, I_b, I_q, I_s, R, V) \in \mathbb{R}_+^{11}, \ N \leq \frac{\Lambda}{\mu_h} \ \text{ and } \ V \leq \frac{r\Lambda}{\mu_v\mu_h}\right\}, \tag{9}$$

is positively invariant and attracting for model (4). Then, it is sufficient to consider the dynamics of the flow generated by model (4) in Ω.

Remark 3.1. : Each maximal solution of model (4) is global.

3.2. Asymptomatic stability of the disease-free equilibrium

Model (4) has a disease-free equilibrium (DFE) obtained by setting the right-hand side of equations in model system (4) to zero with $Q = L = I_a = I_b = I_q = I_s = V = 0$. The disease-free equilibrium is

$$\mathcal{E} = \left(S_0, C_p^0, C_t^0, 0, 0, 0, 0, 0, 0, 0, 0\right) \tag{10}$$

where S_0, C_p^0 and C_t^0 are given by

$$\begin{cases} S_0 = \dfrac{k_3(\mu_h+p_1)+t_2\mu_h}{[k_1t_2+(k_1+p_1)k_3]}\dfrac{\Lambda}{\mu_h}, \\ C_p^0 = \dfrac{p_2k_3}{[k_1t_2+(k_1+p_1)k_3]}\dfrac{\Lambda}{\mu_h}. \\ C_t^0 = \dfrac{p_2t_2}{[k_1t_2+(k_1+p_1)k_3]}\dfrac{\Lambda}{\mu_h}, \end{cases} \tag{11}$$

Note that the total human population at the DFE, $\mathcal{E}$, satisfies

$$N_0 = S_0 + C_p^0 + C_t^0 = \frac{\Lambda}{\mu_h}. \tag{12}$$

The basic reproduction number, which is very important for the qualitative analysis of the model, is determined here below by using the method of the next generation matrix used in van den Driessche and Watmough [44]. Following notations in van den Driessche and Watmough [44], matrices F and V for the new infection terms and the remaining transfer terms are, respectively, given by

$$F = \begin{bmatrix} 0 & \pi\frac{S_0\kappa\beta_h}{N_0} & \pi\frac{S_0\beta_h}{N_0} & \pi\frac{S_0\beta_h}{N_0} & 0 & \pi\frac{S_0\beta_h}{N_0} & 0 \\ 0 & 0 & (1-\pi)\frac{\beta_h(C_p^0\epsilon+S_0)}{N_0} & (1-\pi)\frac{\beta_h(C_p^0\epsilon+S_0)}{N_0} & 0 & (1-\pi)\frac{\beta_h(C_p^0\epsilon+S_0)}{N_0} & (1-\pi)\frac{\beta_v(C_p^0\epsilon+S_0)}{K} \\ 0 & 0 & 0 & 0 & 0 & 0 & 0 \\ 0 & 0 & 0 & 0 & 0 & 0 & 0 \\ 0 & 0 & 0 & 0 & 0 & 0 & 0 \\ 0 & 0 & 0 & 0 & 0 & 0 & 0 \\ 0 & 0 & 0 & 0 & 0 & 0 & 0 \end{bmatrix}$$

and

$$V = \begin{bmatrix} k_4 & 0 & 0 & 0 & 0 & 0 & 0 \\ 0 & k_5 & 0 & 0 & 0 & 0 & 0 \\ 0 & -\omega_a & k_6 & 0 & 0 & 0 & 0 \\ 0 & -\omega_b & 0 & k_7 & 0 & 0 & 0 \\ 0 & 0 & 0 & -\nu_b & k_8 & -\nu_s & 0 \\ 0 & -\omega_s & 0 & -\sigma & 0 & k_9 & 0 \\ 0 & 0 & -r_a & -r_b & 0 & -r_s & \mu_v \end{bmatrix}$$

The basic reproduction number denoted by $\mathcal{R}_0$ is defined as the average number of secondary cases produced in a completely susceptible population by a typical infected individual during its entire period of being infectious [43,44]. Mathematically, $\mathcal{R}_0$ is the spectral radius of the next-generation matrix, FV^{-1}. After further simplification, we obtain

$$\mathcal{R}_0 = (1-\pi)\left[\beta_h\frac{(S_0+\epsilon C_p^0)}{N_0k_5}\left(\frac{\omega_b\sigma}{k_7k_9}+\frac{\omega_s}{k_9}+\frac{\omega_b}{k_7}+\frac{\omega_a}{k_6}\right)+\beta_v\frac{(S_0+\epsilon C_p^0)}{K\mu_vk_5}\left(\frac{\omega_br_s\sigma}{k_7k_9}+\frac{\omega_sr_s}{k_9}+\frac{\omega_br_b}{k_7}+\frac{\omega_ar_a}{k_6}\right)\right] \tag{13}$$

Thanks to Theorem 2 in van den Driessche and Watmough [44], we claim the following result.

Lemma 3.1. *The DFE, $\mathcal{E}$, of model (4) is locally asymptotically stable (LAS) if $\mathcal{R}_0 < 1$ and unstable if $\mathcal{R}_0 > 1$.*

The biological implication of Lemma 3.1 is that a sufficiently small flow of infectious individuals will not generate an outbreak of the disease unless $\mathcal{R}_0 > 1$. For better control of the disease, the global asymptotic stability (GAS) of the DFE is needed. Actually, enlarging the

basin of attraction of $\mathcal{E}$ to be the entire Ω is, for the model under consideration a more challenging task involving relatively new results. We use the result of Kamgang and Sallet [55] for the global stability of the disease-free equilibrium for a class of epidemiological models.

Using the result of Kamgang and Sallet [55], model system (4) can be written in the following form:

$$\begin{cases} \dot{X}_S = \mathcal{A}_1(X)(X_S - X_s^0) + \mathcal{A}_{12}(X)X_I \\ \dot{X}_I = \mathcal{A}_2(X)X_I \end{cases} \tag{14}$$

where X_S represents the class of non infected individuals (S, C_p, C_t) and the vector X_I represents the class of infected individuals (Q, L, I_a, I_b, I_q, I_s, V). Here, we have $X_S = (S, C_p, C_t)^T$, $X_I = (Q, L, I_a, I_b, I_q, I_s, V)^T$, $X = (X_S, X_I)^T$ and $X_s^0 = \left(S_0, C_p^0, C_t^0\right)^T$, with

$$\mathcal{A}_1(X) = \begin{pmatrix} -k_1 & p_1 & 0 \\ p_2 & -k_2 & t_1 \\ 0 & t_2 & -k_3 \end{pmatrix},$$

$$\mathcal{A}_{12}(X) = \begin{pmatrix} q & 0 & \zeta\varphi\beta_h\frac{S}{N} & \zeta\varphi\beta_h\frac{S}{N} & 0 & \zeta\varphi\beta_h\frac{S}{N} & \zeta\varphi\beta_v\frac{S}{V+K} \\ 0 & 0 & -\zeta\epsilon\beta_h\frac{C_p}{N} & -\zeta\epsilon\beta_h\frac{C_p}{N} & 0 & -\zeta\epsilon\beta_h\frac{C_p}{N} & -\zeta\epsilon\beta_v\frac{C_p}{V+K} \\ 0 & 0 & 0 & 0 & 0 & 0 & 0 \end{pmatrix},$$

and

$$\mathcal{A}_2(X) = \begin{pmatrix} -k_4 & \pi\beta_h\kappa\frac{S}{N} & \pi\beta_h\frac{S}{N} & \pi\beta_h\frac{S}{N} & 0 & \pi\beta_h\frac{S}{N} & 0 \\ 0 & -k_5 & \zeta\beta_h\frac{S+\epsilon C_p}{N} & \zeta\beta_h\frac{S+\epsilon C_p}{N} & 0 & \zeta\beta_h\frac{S+\epsilon C_p}{N} & \zeta\beta_v\frac{S+\epsilon C_p}{V+K} \\ 0 & \omega_a & -k_6 & 0 & 0 & 0 & 0 \\ 0 & \omega_b & 0 & -k_7 & 0 & 0 & 0 \\ 0 & 0 & 0 & \nu_b & -k_8 & \nu_s & 0 \\ 0 & \omega_s & 0 & \sigma & 0 & -k_9 & 0 \\ 0 & 0 & r_a & r_b & 0 & r_s & -\mu_v \end{pmatrix},$$

with $\varphi := 1 + \epsilon$ and $\zeta := 1 - \pi$.

A direct computation shows that the eigenvalues of $\mathcal{A}_1(X)$ are real and negative. Thus the system $\dot{X}_S = \mathcal{A}_1(X)(X_S - X_s^0)$ is globally asymptotically stable at the equilibrium $X_s^0 = \left(S_0, C_p^0, C_t^0\right)$. Note also that $\mathcal{A}_2(X)$ is a Metzler matrix, i.e. a matrix such that off diagonal terms are non negative [56,57].

Let us consider the bounded set $\mathcal{D}$:

$$\mathcal{D} = \{(X_S, X_I) \in \Omega, \quad X_S \neq 0\}. \tag{15}$$

Let us recall the following theorem [55]

Theorem 3.2. *Let $\mathcal{D} \subset \mathcal{V} = \mathbb{R}^3 \times \mathbb{R}^7$. The system (14) is of class C^1, defined on $\mathcal{V}$. If*

(1) *$\mathcal{D}$ is positively invariant relative to (14).*
(2) *The system $\dot{X}_S = \mathcal{A}_1(X)(X_S - X_s^0)$ is globally asymptotically stable at the equilibrium $X_s^0 = \left(S_0, C_p^0, C_t^0\right)$ on the canonical projection of $\mathcal{D}$ on $\mathbb{R}^3_+$.*
(3) *For any $x \in \mathcal{D}$, the matrix $\mathcal{A}_2(X)$ is Metzler irreducible.*
(4) *There exists a matrix $\bar{\mathcal{A}}_2$, which is an upper bound of the set $\mathbb{M} = \{\mathcal{A}_2(x) \in \mathcal{M}_4(\mathbb{R}) : x \in \mathcal{D}\}$ with the property that if $\bar{\mathcal{A}}_2 \in \mathbb{M}$, for any $\bar{x} \in \mathcal{D}$, such that $\mathcal{A}_2(\bar{x}) = \bar{\mathcal{A}}_2$, then $\bar{x} \in \mathbb{R}^3 \times \left\{0_{\mathbb{R}^7}\right\}$.*
(5) *The stability modulus of $\bar{\mathcal{A}}_2$,*
$\alpha(\bar{\mathcal{A}}_2) = \max_{\lambda \in sp(\bar{\mathcal{A}}_2)} \mathcal{R}\mathbf{e}(\lambda)$ satisfied $\alpha(\bar{\mathcal{A}}_2) \leq 0$.

Then the DFE is GAS in $\mathcal{D}$. (See [55] for a proof).

Let us now verify the assumptions of the previous theorem: it is obvious that conditions (1–3) of the theorem are satisfied. An upper bound of the set of matrices $\mathcal{A}_2$, which is the matrix $\bar{\mathcal{A}}_2$ is given by

$$\bar{\mathcal{A}}_2 = \begin{pmatrix} -k_4 & \pi\beta_h\kappa & \pi\beta_h & \pi\beta_h & 0 & \pi\beta_h & 0 \\ 0 & -k_5 & \zeta\beta_h & \zeta\beta_h & 0 & \zeta\beta_h & \zeta\beta_v(S_0 + \epsilon C_p^0) \\ 0 & \omega_a & -k_6 & 0 & 0 & 0 & 0 \\ 0 & \omega_b & 0 & -k_7 & 0 & 0 & 0 \\ 0 & 0 & 0 & \nu_b & -k_8 & \nu_s & 0 \\ 0 & \omega_s & 0 & \sigma & 0 & -k_9 & 0 \\ 0 & 0 & r_a & r_b & 0 & r_s & -\mu_v \end{pmatrix},$$

To check condition (5) in Theorem 3.2, we will use the following useful lemma [55] which is the a characterization of Metzler stable matrices:

Lemma 3.2. *Let M be a square Metzler matrix written in block form $\begin{pmatrix} A & B \\ C & D \end{pmatrix}$ with A and D square matrices. M is Metzler stable if and only if matrices A and $D - CA^{-1}B$ are Metzler stable.*

Using Lemma 3.2, matrix $\bar{\mathcal{A}}_2$ can be express in the form of the matrix M with:

$$A=\begin{pmatrix}-k_4 & \pi\beta_h\kappa & \pi\beta_h & \pi\beta_h\\ 0 & -k_5 & \zeta\beta_h & \zeta\beta_h\\ 0 & \omega_a & -k_6 & 0\\ 0 & \omega_b & 0 & -k_7\end{pmatrix},\ B=\begin{pmatrix}0 & \pi\beta_h & 0\\ 0 & \zeta\beta_h & \zeta\beta_v(S_0+\epsilon C_p^0)\\ 0 & 0 & 0\\ 0 & 0 & 0\end{pmatrix},\ C=\begin{pmatrix}0 & 0 & 0 & \nu_b\\ 0 & \omega_s & 0 & \sigma\\ 0 & 0 & r_a & r_b\end{pmatrix}\text{ and}$$

$$D=\begin{pmatrix}-k_8 & \nu_s & 0\\ 0 & -k_9 & 0\\ 0 & r_s & -\mu_v\end{pmatrix}.$$

Clearly, A is a stable Metzler matrix. Then, after some computations, we obtain $D-CA^{-1}B$ is a stable Metzler matrix if and only if

$$\mathcal{R}_0^{max}=(1-\pi)\frac{1}{k_5}\left[\beta_h\left(\frac{\omega_b\sigma}{k_7k_9}+\frac{\omega_s}{k_9}+\frac{\omega_b}{k_7}+\frac{\omega_a}{k_6}\right)+\beta_v\frac{(S_0+\epsilon C_p^0)}{\mu_v}\left(\frac{\omega_br_s\sigma}{k_7k_9}+\frac{\omega_sr_s}{k_9}+\frac{\omega_br_b}{k_7}+\frac{\omega_ar_a}{k_6}\right)\right]\le 1 \tag{16}$$

Thus we claim the following result

Theorem 3.3. *If $\mathcal{R}_0^{\max}\le 1$, then the disease-free equilibrium $\mathcal{E}$ is globally asymptotically stable in $\mathcal{D}$.*

Remark 3.2. Note that the condition (16) is equivalent to

$$\mathcal{R}_0\le\mathcal{R}_c=\frac{(S_0+\epsilon C_p^0)}{KN_0}\frac{\beta_hK\mu_\nu R_1+\beta_\nu N_0R_2}{\beta_h\mu_\nu R_1+\beta_\nu(S_0+\epsilon C_p^0)R_2} \tag{17}$$

where $R_1=\frac{\omega_b\sigma}{k_7k_9}+\frac{\omega_s}{k_9}+\frac{\omega_b}{k_7}+\frac{\omega_a}{k_6}$ and $R_2=\frac{\omega_br_s\sigma}{k_7k_9}+\frac{\omega_sr_s}{k_9}+\frac{\omega_br_b}{k_7}+\frac{\omega_ar_a}{k_6}$

Theorem (3.3) means that for $\mathcal{R}_0<\mathcal{R}_c\le 1$, the DFE $\mathcal{E}$ is the unique equilibrium in $\mathcal{D}$ which is GAS. If $\mathcal{R}_c<\mathcal{R}_0\le 1$, the backward bifurcation phenomenon may occurs in Ω, i.e. the DFE $\mathcal{E}$, may coexists with two endemic equilibrium, one asymptotically stable and one unstable.

The epidemiological significance of the phenomenon of backward bifurcation is that the requirement of $\mathcal{R}_c<\mathcal{R}_0<1$ is, although necessary, no longer sufficient for disease eradication when the initial condition is taken in Ω. In such a scenario, disease elimination would depend on various initial sizes of the population (state variables) chosen Ω. That is, the presence of backward bifurcation in the *COVID-19* transmission model (4) suggests that the feasibility of controlling *COVID-19* when $\mathcal{R}_c<\mathcal{R}_0<1$ always be dependent on the initial sizes of the population even if they are chosen in Ω.

To confirm whether or not the backward bifurcation phenomenon occurs in this case, one could use the approach developed in van den Driessche and Watmough [44], Castillo-Chavez and Song [59], which is based on the general centre manifold theory [58].

Theorem 3.4. *The model (4) undergoes a backward bifurcation at $\mathcal{R}_0=1$ when the parameters satisfy the condition*

$$\frac{A_1+A_2}{A_3}<1, \tag{18}$$

where

$$A_1=2\zeta(\chi_1\chi_6+\chi_1\chi_7+\chi_1\chi_9)\frac{\beta_h}{N_0^2}((1-\varepsilon)C_p^0+C_t^0)+2\zeta\varepsilon(\chi_2\chi_6+\chi_2\chi_7+\chi_2\chi_9)C_t^0\frac{\beta_h}{N_0^2}+2\zeta\chi_{11}\frac{\beta_\nu}{K}(\chi_1+\varepsilon\chi_2),$$

$$A_2=2\zeta(2\chi_6\chi_7+2\chi_6\chi_9+2\chi_7\chi_9+\chi_6^2+\chi_7^2+\chi_9^2)\times\frac{(S_0+\varepsilon C_p^0)}{N_0^2}+\zeta\chi_{11}^2\frac{2\beta_\nu(S_0+\varepsilon C_p^0)}{K^2},$$

$$A_3=2\zeta\frac{(1-\varepsilon)\beta_hS_0}{N_0^2}(\chi_2\chi_6+\chi_2\chi_7+\chi_2\chi_9).$$

Proof: The theorem is the direct application of Theorem 4.1 in Castillo-Chavez and Song [59]. To check the existence of backward bifurcation of the model (4) at $\mathcal{R}_0=1$, we use the center manifold theorem [58]. For this purpose, we introduce the following change of variables.

$$S=x_1,\ C_p=x_2,\ C_t=x_3,\ Q=x_4,\ L=x_5,\ I_a=x_6,\ I_b=x_7,\ I_q=x_8,\ I_s=x_9,\ R=x_{10}\ \text{ and }\ V=x_{11} \tag{19}$$

so that

$$N=x_1+x_2+x_3+x_4+x_5+x_6+x_7+x_8+x_9+x_{10},\ \lambda_s=(1-\pi)\left[\beta_h\frac{x_6+x_7+x_9}{N}+\beta_\nu\frac{x_{11}}{x_{11}+K}\right]$$

$$\lambda_p=\epsilon\lambda_s\ \text{ and }\ \lambda_q=\pi\beta_h\frac{\kappa x_5+x_6+x_7+x_9}{N}$$

Further, by using the vector notation $x=(x_1,x_2,x_3,x_4,x_5,x_6,x_7,x_8,x_9,x_{10},x_{11})^T$, model (4) can be written in the form $\dot{x}=f(x)$ with $f=(f_1,f_2,f_3,f_4,f_5,f_6,f_7,f_8,f_9,f_{10},f_{11})^T$ as follows:

$$\begin{cases}\dot{x_1}=\Lambda+qx_4+p_1x_2-(\lambda_q+\lambda_s+k_1)x_1,\\ \dot{x_2}=p_2x_1+t_1x_3-(\lambda_p+k_2)x_2,\\ \dot{x_3}=t_2x_2-k_3x_3,\\ \dot{x_4}=\lambda_qx_1-k_4x_4,\\ \dot{x_5}=\lambda_sx_1+\lambda_px_2-k_5x_5,\\ \dot{x_6}=\omega_ax_5-k_6x_6\\ \dot{x_7}=\omega_bx_5-k_7x_7\\ \dot{x_8}=\nu_bx_7+\nu_sx_9-k_8x_8\\ \dot{x_9}=\omega_sx_5+\sigma x_7-k_9x_9\\ \dot{x_{10}}=+\alpha_qx_4+\alpha_ax_6+\alpha_bx_7+\alpha_ix_8+\alpha_sx_9-\mu_hR\\ \dot{x_{11}}=r_ax_6+r_bx_7+r_sx_9-\mu_\nu x_{11}\end{cases} \tag{20}$$

The Jacobian of system (20) at the DFE $\mathcal{E}$ is

$$J=\begin{bmatrix}
-k_1 & p_1 & 0 & q & -\frac{\pi\beta_h\kappa S_0}{N_0} & -\frac{\beta_h S_0}{N_0} & -\frac{\beta_h S_0}{N_0} & 0 & -\frac{\beta_h S_0}{N_0} & 0 & -\frac{(1-\pi)\beta_v S_0}{K}\\
p_2 & -k_2 & t_1 & 0 & 0 & -\frac{\varepsilon\zeta\beta_h C_p^0}{N_0} & -\frac{\varepsilon\zeta\beta_h C_p^0}{N_0} & 0 & -\frac{\varepsilon\zeta\beta_h C_p^0}{N_0} & 0 & -\frac{\varepsilon\zeta\beta_v C_p^0}{K}\\
0 & t_2 & -k_3 & 0 & 0 & 0 & 0 & 0 & 0 & 0 & 0\\
0 & 0 & 0 & -k_4 & \frac{\pi\beta_h\kappa S_0}{N_0} & \frac{\pi\beta_h S_0}{N_0} & \frac{\pi\beta_h S_0}{N_0} & 0 & \frac{\pi\beta_h S_0}{N_0} & 0 & 0\\
0 & 0 & 0 & 0 & -k_5 & \frac{\zeta\beta_h(S_0+\varepsilon C_p^0)}{N_0} & \frac{\zeta\beta_h(S_0+\varepsilon C_p^0)}{N_0} & 0 & \frac{\zeta\beta_h(S_0+\varepsilon C_p^0)}{N_0} & 0 & \frac{\zeta\beta_v(S_0+\varepsilon C_p^0)}{K}\\
0 & 0 & 0 & 0 & \omega_a & -k_6 & 0 & 0 & 0 & 0 & 0\\
0 & 0 & 0 & 0 & \omega_b & 0 & -k_7 & 0 & 0 & 0 & 0\\
0 & 0 & 0 & 0 & 0 & 0 & \nu_b & -k_8 & \nu_s & 0 & 0\\
0 & 0 & 0 & 0 & \omega_s & 0 & \sigma & 0 & -k_9 & 0 & 0\\
0 & 0 & 0 & \alpha_q & 0 & \alpha_a & \alpha_b & \alpha_i & \alpha_s & -\mu_h & 0\\
0 & 0 & 0 & 0 & 0 & r_a & r_b & 0 & r_s & 0 & -\mu_v
\end{bmatrix}.$$

where $\zeta = 1-\pi$.

The basic reproduction number of the transformed (linearized) model system (20) is the same as that of the original model given by Eq. (4). Therefore, choosing β_h as a bifurcation parameter by solving for π when $\mathcal{R}_0 = 1$, one obtains

$$\beta_h^* = \left[\frac{1}{1-\pi} - \beta_v\frac{(S_0+\epsilon C_p^0)}{K\mu_v k_5}\left(\frac{\omega_b r_s\sigma}{k_7k_9}+\frac{\omega_s r_s}{k_9}+\frac{\omega_b r_b}{k_7}+\frac{\omega_a r_a}{k_6}\right)\right]\left[\frac{(S_0+\epsilon C_p^0)}{N_0k_5}\left(\frac{\omega_b\sigma}{k_7k_9}+\frac{\omega_s}{k_9}+\frac{\omega_b}{k_7}+\frac{\omega_a}{k_6}\right)\right]^{-1} \tag{21}$$

It follows that the Jacobian $J(\mathcal{E})$ of system (20) at the DFE $\mathcal{E}$, with $\beta_h = \beta_h^*$, denoted by $J_{\beta_h^*}$ has a simple zero eigenvalue (with all other eigenvalues having negative real parts). Hence, the Center Manifold theory [58] can be used to analyze the dynamics of the system (20). In particular, the theorem in Castillo and Song [59], reproduced below for convenience, will be used to show that when $\mathcal{R}_0 > 1$ there exists an endemic equilibrium of system (20) which is locally asymptotically stable for $\mathcal{R}_0$ near 1 under certain conditions.

Theorem 3.5. *(Castillo-Chavez and Song [59]): Consider the following general system of ordinary differential equations with a parameter Φ:*

$$\frac{dz}{dt} = f(x,\Phi),\ f:\mathbb{R}^n\times\mathbb{R} \quad \text{and} \quad f\in C^2(\mathbb{R}^n,\mathbb{R}), \tag{22}$$

where 0 is an equilibrium point of the system (that is, $f(0,\Phi)\equiv 0$ for all Φ) and assume

1. *$A = D_z f(0,0) = \left(\frac{\partial f_i}{\partial z_j}(0,0)\right)$ is the linearization matrix of system (22) around the equilibrium 0 with Φ evaluated at 0. Zero is a simple eigenvalue of A and other eigenvalues of A have negative real parts;*
2. *Matrix A has a right eigenvector u and a left eigenvector v (each corresponding to the zero eigenvalue). Let f_k be the k^{th} component of f and*

$$a = \sum_{k,i,j=1}^{n} v_k u_i u_j \frac{\partial^2 f_k}{\partial x_i \partial x_j}(0,0) \quad \text{and} \quad b = \sum_{k,i=1}^{n} v_k u_i \frac{\partial^2 f_k}{\partial x_i \partial \Phi}(0,0),$$

then, the local dynamics of the system around the equilibrium point 0 is totally determined by the signs of a and b.

1. *$a>0$, $b>0$. When $\Phi<0$ with $|\Phi|\ll 1$, 0 is locally asymptotically stable and there exists a positive unstable equilibrium; when $0<\Phi\ll 1$, 0 is unstable and there exists a negative, locally asymptotically stable equilibrium;*
2. *$a<0$, $b<0$. When $\Phi<0$ with $|\Phi|\ll 1$, 0 is unstable; when $0<\Phi\ll 1$, 0, is locally asymptotically stable equilibrium, and there exists a positive unstable equilibrium;*
3. *$a>0$, $b<0$. When $\Phi<0$ with $|\Phi|\ll 1$, 0 is unstable and there exists a locally asymptotically stable negative equilibrium; when $0<\Phi\ll 1$, 0 is stable, and a positive unstable equilibrium appears;*
4. *$a<0$, $b>0$. When Φ changes from negative to positive, 0 changes its stability from stable to unstable. Correspondingly a negative unstable equilibrium becomes positive and locally asymptotically stable.*

In order to apply the above theorem, the following computations are necessary (it should be noted that we are used β_h^* as the bifurcation parameter, in place of Φ in Theorem 3.5).

Eigenvectors of $J_{\beta_h^*}$: For the case when $\mathcal{R}_0 = 1$, it can be shown that the Jacobian of system (20) has a right eigenvector $U = (u_1,u_2,u_3,u_4,u_5,u_6,u_7,u_8,u_9,u_{10},u_{11})^T$ verifying $J_{\beta_h^*}U = 0$ given by:

$$u_1 = -\chi_1 u_5,\ u_2 = -\chi_2 u_5,\ u_3 = \chi_3 u_5,\ u_4 = \chi_4 u_5,\ u_5 = u_5 > 0,\ u_6 = \chi_6 u_5,\ u_7 = \chi_7 u_5,\ u_8 = \chi_8 u_5,\ u_8 = \chi_8 u_5$$

$$u_9 = \chi_9 u_5,\ u_{10} = \chi_{10} u_5, \text{ and } u_{11} = \chi_{11} u_5$$

where

$$\chi_6 = \frac{\omega_a}{k_6},\ \chi_7 = \frac{\omega_b}{k_7},\ \chi_8 = \frac{1}{k_8}\left(\frac{\nu_b\omega_b}{k_7}+\frac{\nu_s\omega_s}{k_9}+\frac{\nu_s\sigma\omega_b}{k_7k_9}\right),\ \chi_9 = \frac{1}{k_9}\left(\omega_s+\frac{\sigma\omega_b}{k_7}\right)$$

$$\chi_{11} = \frac{1}{\mu_v}\left(\frac{r_a\omega_a}{k_6}+\frac{r_b\omega_b}{k_7}+\frac{r_s\omega_s}{k_9}+\frac{r_s\sigma\omega_b}{k_7k_9}\right),\ \chi_4 = \frac{\pi\beta_h S_0}{k_4N_0}\left(\kappa+\frac{\omega_b\sigma}{k_7k_9}+\frac{\omega_s}{k_9}+\frac{\omega_b}{k_7}+\frac{\omega_a}{k_6}\right)$$

$$\chi_{10} = \frac{1}{\mu_h}\left(\alpha_q\chi_4+\alpha_a\chi_6+\alpha_b\chi_7+\alpha_i\chi_8+\alpha_s\chi_9\right),$$

$$\chi_1 = \frac{1}{\Delta}\left[\Gamma\left(\Psi\chi_4 + \frac{\zeta\beta_h S_0}{N_0}(\chi_6+\chi_7+\chi_9) + \frac{\zeta\beta_v S_0}{K}\chi_{11}\right) + p_1\varepsilon\zeta C_p^0\left(\frac{\beta_h}{N_0}(\chi_6+\chi_7+\chi_9) + \frac{\beta_v}{K}\chi_{11}\right)\right]$$

$$\chi_2 = \frac{1}{\Delta}\left[p_2\left(\Psi\chi_4 + \frac{\zeta\beta_h S_0}{N_0}(\chi_6+\chi_7+\chi_9)\right) + k_1\varepsilon\zeta C_p^0\left(\frac{\beta_h}{N_0}(\chi_6+\chi_7+\chi_9) + \frac{\beta_v}{K}\chi_{11}\right)\right] \text{ and } \chi_3 = \frac{t_2}{k_3}\chi_2$$

$$\text{with } \Delta = \frac{k_1k_2k_3 - k_1t_1t_2 - p_1p_2k_3}{k_3} > 0,\ \Gamma = k_2 - \frac{t_1t_2}{k_3} > 0 \text{ and } \Psi = k_4 - q > 0.$$

Similarly, the components of the left eigenvectors $V = (v_1, v_2, v_3, v_4, v_5, v_6, v_7, v_8, v_9, v_{10}, v_{11})$ of $J_{\beta_h^*}$ verifying $VJ_{\beta_h^*} = 0$ are given by

$$v_1 = 0,\ v_2 = 0,\ v_3 = 0,\ v_4 = 0,\ v_5 = v_5 > 0,\ v_6 = \vartheta_6 v_5,\ v_7 = \vartheta_7 v_5,\ v_8 = 0,\ v_9 = \vartheta_9 v_5,\ v_{10} = 0 \text{ and } v_{11} = \vartheta_{11} v_5$$

where

$$\vartheta_6 = \frac{1}{k_6}\left(A + \frac{Br_a}{\mu_v}\right),\ \vartheta_7 = \frac{1}{k_7}\left(A + \frac{\sigma}{k_9}\left(A + \frac{Br_s}{\mu_v}\right) + \frac{Br_b}{\mu_v}\right),\ \vartheta_9 = \frac{1}{k_9}\left(A + \frac{Br_s}{\mu_v}\right) \text{ and } \vartheta_{11} = \frac{B}{\mu_v}$$

$$\text{with } A = \frac{(1-\pi)\beta_h(S_0 + \varepsilon C_p^0)}{N_0} \text{ and } B = \frac{(1-\pi)\beta_v(S_0 + \varepsilon C_p^0)}{K}$$

Computation of a: The bifurcation coefficient a at the DFE is given by

$$\begin{aligned} a &= \sum_{i,j,k=1}^{11} v_k u_i u_j \frac{\partial^2 f_k}{\partial x_i \partial x_j}(\mathcal{E}_0, \beta_h^*), \\ &= 2v_5\left(u_1u_6\frac{\partial^2 f_5}{\partial x_1\partial x_6} + u_1u_7\frac{\partial^2 f_5}{\partial x_1\partial x_7} + u_1u_9\frac{\partial^2 f_5}{\partial x_1\partial x_9} + u_1u_{11}\frac{\partial^2 f_5}{\partial x_1\partial x_{11}}\right) \\ &\quad + 2v_5\left(u_2u_6\frac{\partial^2 f_5}{\partial x_2\partial x_6} + u_2u_7\frac{\partial^2 f_5}{\partial x_2\partial x_7} + u_2u_9\frac{\partial^2 f_5}{\partial x_2\partial x_9} + u_2u_{11}\frac{\partial^2 f_5}{\partial x_2\partial x_{11}}\right) \\ &\quad + 2v_5\left(u_6u_7\frac{\partial^2 f_5}{\partial x_6\partial x_7} + u_6u_9\frac{\partial^2 f_5}{\partial x_6\partial x_9} + u_7u_9\frac{\partial^2 f_5}{\partial x_7\partial x_9}\right) \\ &\quad + v_5\left(u_6u_6\frac{\partial^2 f_5}{\partial x_6\partial x_6} + u_7u_7\frac{\partial^2 f_5}{\partial x_7\partial x_7} + u_9u_9\frac{\partial^2 f_5}{\partial x_9\partial x_9} + u_{11}u_{11}\frac{\partial^2 f_5}{\partial x_{11}\partial x_{11}}\right), \\ &= [-(A_1+A_2)+A_3]v_5u_5^2, \end{aligned}$$

where

$$A_1 = 2\zeta(\chi_1\chi_6 + \chi_1\chi_7 + \chi_1\chi_9)\frac{\beta_h}{N_0^2}((1-\varepsilon)C_p^0 + C_t^0) + 2\zeta\varepsilon(\chi_2\chi_6 + \chi_2\chi_7 + \chi_2\chi_9)C_t^0\frac{\beta_h}{N_0^2} + 2\zeta\chi_{11}\frac{\beta_v}{K}(\chi_1 + \varepsilon\chi_2),$$

$$A_2 = 2\zeta(2\chi_6\chi_7 + 2\chi_6\chi_9 + 2\chi_7\chi_9 + \chi_6^2 + \chi_7^2 + \chi_9^2) \times \frac{(S_0 + \varepsilon C_p^0)}{N_0^2} + \zeta\chi_{11}^2\frac{2\beta_v(S_0 + \varepsilon C_p^0)}{K^2},$$

$$A_3 = 2\zeta\frac{(1-\varepsilon)\beta_h S_0}{N_0^2}(\chi_2\chi_6 + \chi_2\chi_7 + \chi_2\chi_9).$$

Thus,

$$a > 0 \iff \tfrac{A_1+A_2}{A_3} < 1. \tag{23}$$

Computation of b: The second bifurcation coefficient b is given by

$$\begin{aligned} b &= v_5u_6\tfrac{\partial f_5}{\partial x_6\partial\beta_h}(0,\beta_h^*) + v_5u_7\tfrac{\partial f_5}{\partial x_7\partial\beta_h}(0,\beta_h^*) + v_5u_9\tfrac{\partial f_5}{\partial x_9\partial\beta_h}(0,\beta_h^*), \\ &= (1-\pi)\tfrac{S_0+\epsilon C_p^0}{N_0}(\chi_6+\chi_7+\chi_9)u_5v_5 > 0. \end{aligned}$$

Thus, depending on the values of the parameters of the model system (4), the value of a can be positive or negative. So, if $b > 0$, if $a > 0$, model system (4) undergoes the phenomenon of backward bifurcation (see Theorem 3.5, item (1)). Also, if $a < 0$ (by Theorem 3.5, item (4)), we have established the result about the local stability of the endemic equilibrium of model system (4) for $\mathcal{R}_0^0 > 1$ but close to 1. This concludes the proof of Theorem 3.4□

4. Numerical simulation

4.1. Sensitivity analysis of model's parameters

The sensitivity analysis of the model parameters done in this section aims to measure firstly the correlation between model's parameters (4) and state variables of infected people (see Table 2) and secondly the correlation between model's parameters (4) and threshold parameters $\mathcal{R}_0$, $\mathcal{R}_0^{\max}$ and $\mathcal{R}_c$ (see Table 5). After this, we compute the sensitivity index of threshold parameters $\mathcal{R}_0$, $\mathcal{R}_0^{\max}$ and $\mathcal{R}_c$ with respect to model's parameters (4).

Table 2
Table of parameters PRCCs with model's variables .

Parameters	Range	Q	I_b	I_a	I_q	I_s	V
Λ	[1–300]	0.1831	0.1852	0.1843	0.0053	0.3033	0.0076
μ_h	[0.001–0.999]	−0.0022	0.0605	0.0023	−0.1409	0.0600	0.1167
β_h	[0.001–0.999]	0.6824**	0.5938**	0.6105**	0.6789**	0.5557**	0.6269**
β_v	[0.001–0.999]	0.0088	−0.1213	−0.0573	0.0010	0.0106	0.0585
q	[0.001–0.999]	0.1424	0.0493	0.2514	−0.0128	0.1226	−0.0175
p_2	[0.001–0.999]	−0.5764**	−0.2188	−0.5455	−0.3697	−0.3160	−0.2981
t_2	[0.001–0.999]	0.0132	−0.0113	−0.0888	0.0391	−0.0329	−0.2615
p_1	[0.001–0.999]	0.1641	0.0893	0.1295	0.0286	−0.0643	0.2058
t_1	[0.001–0.999]	0.0611	−0.0583	0.0500	0.0774	−0.1312	0.2500
d_1	[0.001–0.999]	−0.0916	0.0074	0.0222	0.0628	0.1065	0.0749
d_2	[0.001–0.999]	0.0125	−0.1768	0.0716	−0.1505	−0.3062	−0.2022
K	[1–10^6]	0.1961	−0.1444	0.1738	−0.2030	0.0651	0.0613
ω_a	[0.001–0.999]	0.0003	0.0823	0.0369	0.2173	0.2012	0.2489
ω_b	[0.001–0.999]	−0.1710	−0.0435	−0.2703	0.0940	0.0333	0.2163
ω_s	[0.001–0.999]	−0.2521	0.2470	−0.2028	0.0030	−0.0061	0.2105
r_a	[0.001–0.999]	−0.0348	0.0974	−0.0991	0.0046	0.0206	0.1799
r_b	[0.001–0.999]	0.1102	0.2058	0.0994	0.0426	−0.0131	−0.0968
r_s	[0.001–0.999]	0.0077	0.2037	0.0209	−0.0760	0.0512	−0.0922
μ_v	[0.001–0.999]	−0.1160	−0.1748	−0.0815	−0.3193	−0.1794	−0.5602**
σ	[0.001–0.999]	−0.0784	0.0458	−0.0606	−0.0406	−0.0634	−0.0583
ν_b	[0.001–0.999]	−0.2623	−0.2684	−0.2651	−0.1645	−0.2862	−0.1951
ν_s	[0.001–0.999]	−0.2835	−0.2042	−0.3002	−0.1475	−0.3459	−0.0756
α_a	[0.001–0.999]	−0.6206**	−0.5275**	−0.6745**	−0.5161**	−0.5679**	−0.5631**
α_b	[0.001–0.999]	0.0048	−0.1706	−0.0141	−0.1300	−0.2197	0.0263
α_s	[0.001–0.999]	−0.3293	−0.1252	−0.2688	−0.0716	−0.1597	−0.0186
α_i	[0.001–0.999]	0.0115	−0.0784	−0.0019	−0.0635	0.2158	−0.0667
α_q	[0.001–0.999]	−0.1010	0.0555	−0.0444	0.0879	0.0593	-0.0041**
π	[0.001–0.999]	−0.0332	−0.1896	−0.4553	−0.2007	−0.2916	−0.2705
ϵ	[0.001–0.999]	0.2893	0.1999	0.0347	0.2489	0.2634	0.0548
κ	[0.001–0.999]	−0.0361	0.1355	−0.0285	0.0635	−0.0335	−0.2624

**: p-value $<$ 0.001.

Table 3
List of parameters statistically more influencing to state variables Q, I_a, I_b, I_q and I_s.

Variables	Q	I_b	I_a	I_q	I_s	V
Correlated parameters significantly	β_h, α_a, p_2	β_h, α_a	β_h, α_a	β_h, α_a	β_h, α_a	β_h, α_a, μ_v

We compute the partial ranking correlation coefficient (PRCC) of parameters against the model's variables Q, I_a, I_b, I_q, I_s and V. A positive (negative) correlation coefficient corresponds to an increasing (decreasing) monotonic trend between the model's variable and the parameter under consideration.

The results in Table 2 show values of PRCCs at time $t = 3000$ days of simulation. Each row in the table contains the coefficients for the corresponding parameter against the variables in columns. Note that, one parameter in Table 2 is said "significantly correlated to one state variable" if absolute value of PRCC is more than 0.5 and $p - value < 0.001$. We present in Table 3 the list of parameters which are significantly correlated to state variable Q, I_a, I_b, I_q, I_s and V of model (4).

The parameters β_h (exposure rate to infected people) and α_a (recovery rate of asymptomatic infected people) are those significantly correlated to state variables Q, I_a, I_b, I_q, I_s which are related to infected people. This suggests that an effective control strategy should aim to reduce significantly human contact and to quickly identify asymptomatic infected people in order to isolate and treat them.

The relevance of the basic reproduction ratio of $\mathcal{R}_0$ is due to the Lemma 3.1. It is one important key parameter for controlling the disease. The parameters $\mathcal{R}_0^{\max}$ and $\mathcal{R}_c$ are also important to determine conditions of the global stability of DFE. From the previously sampled parameter values, we compute the PRCC between $\mathcal{R}_0$, $\mathcal{R}_0^{\max}$ and $\mathcal{R}_c$ and each parameter of the model (4). The parameters with large PRCC values (> 0.5 or < -0.5) statistically have the most influence [60]. The straightforward computations give on Table 4 the results concerning computation of parameter PRCCs with $\mathcal{R}_0$, $\mathcal{R}_0^{\max}$ and $\mathcal{R}_c$ thresholds.

On Table 5 we give the list of parameters of model (4) more correlated to $\mathcal{R}_0$, $\mathcal{R}_0^{\max}$ and $\mathcal{R}_c$.

It is clear that the parameter β_h is the one-parameter strongly correlated to $\mathcal{R}_0$, $\mathcal{R}_0^{\max}$ and $\mathcal{R}_c$.

The previous computation (PRCC) give us the parameters correlated to $\mathcal{R}_0$, $\mathcal{R}_0^{\max}$ and $\mathcal{R}_c$. We want now to evaluate quantitatively how the parameters of the model can increase or decrease the values of threshold quantities $\mathcal{R}_0$, $\mathcal{R}_0^{\max}$ and $\mathcal{R}_c$. This should be useful to identify the parameters that should be taken into consideration when considering an intervention strategy. Since the parameters $\mathcal{R}_0$, $\mathcal{R}_0^{\max}$ and $\mathcal{R}_c$ are differentiable functions of the parameters, the sensitivity index may alternatively be defined using partial derivatives. For instance, the computation of the sensitivity index of $\mathcal{R}_0$ with respect to p is defined as follows:

$$\Upsilon_p^{\mathcal{R}_0} = \frac{\partial \mathcal{R}_0}{\partial p} \cdot \frac{p}{\mathcal{R}_0}. \tag{24}$$

The result concerning the computation of the sensitivity index of $\mathcal{R}_0$, $\mathcal{R}_0^{\max}$ and $\mathcal{R}_c$ with respect to each parameter is given in the Table 6.

The parameters whose sensitivity index has negative sign decrease the value of the corresponding threshold as their values increase, while those with positive sensitivity index increase the value of the corresponding threshold as they increase. For instance, if the parameter value of ϵ increase for 10% then the value of $\mathcal{R}_0$ will increase for 4.9%. We summarize in Table 7 the list of model's

Table 4
Parameter PRCCs with $\mathcal{R}_0$, $\mathcal{R}_0^{max}$ and $\mathcal{R}_c$ thresholds.

Parameters	$\mathcal{R}_0$	$\mathcal{R}_0^{max}$	$\mathcal{R}_c$	Parameters	$\mathcal{R}_0$	$\mathcal{R}_0^{max}$	$\mathcal{R}_c$
Λ	0.0137	0.5705**	−0.5264**	r_a	0.0130	0.0286	−0.0721
μ_h	0.0684	−0.6773**	0.6694**	r_b	0.0088	−0.3682	−0.3183
β_h	0.8974**	−0.0170	0.6726**	r_s	0.0069	−0.4158	−0.3827
β_v	0.0384	−0.7127**	0.6714**	μ_v	−0.0584	−0.7264**	0.6762**
q	0.0257	−0.0049	−0.0038	σ	−0.2001	0.0089	−0.0952
p_2	−0.5532**	−0.2940	−0.0201	ν_b	−0.3940	−0.2301	0.0345
t_2	−0.0276	−0.0240	0.0064	ν_s	−0.3125	−0.2131	0.0956
p_1	0.2737	0.1207	−0.0264	α_a	−0.4591	−0.0258	−0.1303
t_1	0.0395	0.0217	−0.0287	α_b	−0.1017	−0.0807	0.0003
d_1	−0.0190	−0.0031	−0.0032	α_s	−0.0392	−0.0011	0.0528
d_2	−0.2010	0.1520	0.0518	α_i	−0.0259	0.0035	0.0338
K	−0.0324	−0.0038	−0.0378	α_q	0.0027	0.0351	0.0094
ω_a	0.2468	−0.0604	0.1363	π	−0.0968	−0.0318	0.0246
ω_b	−0.1974	0.0615	−0.1442	ϵ	0.4636	0.2300	0.0132
ω_s	−0.0717	0.0369	−0.0662	κ	0.0192	−0.0329	−0.0350

Table 5
List of parameters more correlated to $\mathcal{R}_0$, $\mathcal{R}_0^{max}$ and $\mathcal{R}_c$.

Thresholds	$\mathcal{R}_0$	$\mathcal{R}_0^{max}$	$\mathcal{R}_c$
Correlated parameters significantly	β_h, p_2	Λ, μ_h, β_v, μ_v	Λ, μ_h, $\beta_h\beta_v\mu_v$,

Table 6
Sensitivity index of threshold parameters $\mathcal{R}_0$, $\mathcal{R}_0^{max}$ and $\mathcal{R}_c$.

Parameters	$\mathcal{R}_0$	$\mathcal{R}_0^{max}$	$\mathcal{R}_c$	Parameters	$\mathcal{R}_0$	$\mathcal{R}_0^{max}$	$\mathcal{R}_c$
Λ	5.4477e−04	0.9972	−0.9967	r_a	2.0335e−05	0.0372	−0.0372
μ_h	0.0164	−0.9714	0.9878	r_b	2.3323e−04	0.4269	−0.4267
β_h	0.9995	0.0028	0.9967	r_s	2.9120e−04	0.5331	−0.5328
β_v	5.4477e−04	0.9972	−0.9967	μ_v	−5.4477e−04	−0.9972	0.9967
q	0	0	0	σ	−0.1209	−3.1577e−05	−0.1209
p_2	−0.1730	−0.1725	−4.7990e−04	ν_b	−0.2596	−0.3050	0.0455
t_2	−0.0139	−0.0139	−3.8573e−05	ν_s	−0.1514	−0.2666	0.1152
p_1	0.0837	0.0835	2.3232e−04	α_a	−0.1841	−0.0329	−0.1512
t_1	0.0103	0.0103	2.8643e−05	α_b	−0.0779	−0.0915	0.0136
d_1	0	0	0	α_s	−0.0324	−0.0571	0.0247
d_2	−0.1081	−0.1904	0.0823	α_i	0	0	0
K	−5.4477e−04	0	−5.4477e−04	α_q	0	0	0
ω_a	0.1125	−0.0612	0.1737	π	−0.996	−0.999	−0.996
ω_b	−0.0640	0.0635	−0.1275	ϵ	0.4919	0.4906	0.0014
ω_s	−0.0383	0.0079	−0.0462	κ	0	0	0

Table 7
List of parameters more affecting $\mathcal{R}_0$, $\mathcal{R}_0^{max}$ and $\mathcal{R}_c$.

Thresholds	$\mathcal{R}_0$	$\mathcal{R}_0^{max}$	$\mathcal{R}_c$
Parameters significantly affecting	β_h, π	Λ, μ_h, β_v, μ_v, r_s, π	Λ, μ_h, β_h, β_v, r_s, π

parameters which significantly affect (sensitivity index > 0.5 or < -0.5) the threshold parameters $\mathcal{R}_0$, $\mathcal{R}_0^{max}$ and $\mathcal{R}_c$.

It is clearly observed from Table 7 that the parameter π and β_h are those modify quickly the threshold parameters $\mathcal{R}_0$, $\mathcal{R}_0^{max}$ and $\mathcal{R}_c$. This means that it is firstly urgent for Cameroonian authorities to improve strategies to identify exposed people in order to isolate them. Secondly, maximise the strategies to reduce human and environmental transmission.

4.2. General dynamics

Numerical simulations using a set of reasonable parameter values in Table 1 is carried out to support analytical results and to evaluate numerically efficiency of control strategies.

The Fig. 2 illustrate global stabilities of disease equilibrium of model (4) using various initial conditions when $\Lambda = 10$, $K = 10^6$ (so that $\mathcal{R}_0 = 0.6910 < 1$). All other parameter values are as in Table 1. As it is expected the solutions of (4) converge toward disease equilibrium.

The Fig. 3 shows time series of model (4) using various initial condition when $\Lambda = 100$, $K = 10^3$ (so that $R_0 = 4.01 > 1$) and all other parameters are as in Table 1. As it is expected the solutions of (4) converge toward endemic equilibrium.

4.3. Impact of controls strategies

Now, numerical simulations are carried out to investigate the impact of control strategies well known and actually applied over the world:

Isolation: It is important to isolate exposed people, individuals traveling from affected countries or potential carriers as it is applied carefully by Cameroonian authorities. This control strategy increases the value of parameter π which concerns the proportion of infectious contact identified. We simulated a model (4) for $\pi = 0.8(\mathcal{R}_0 = 0.89)$, $\pi = 0.6(\mathcal{R}_0 = 1.78)$ and $\pi = 0.5(\mathcal{R}_0 = 2.22)$ when $\Lambda = 100$, $K = 10^3$ and all other parameters values are as in Table 1. As we can see in Fig. 4, isolation has a real impact on *COVID-19* transmission. When

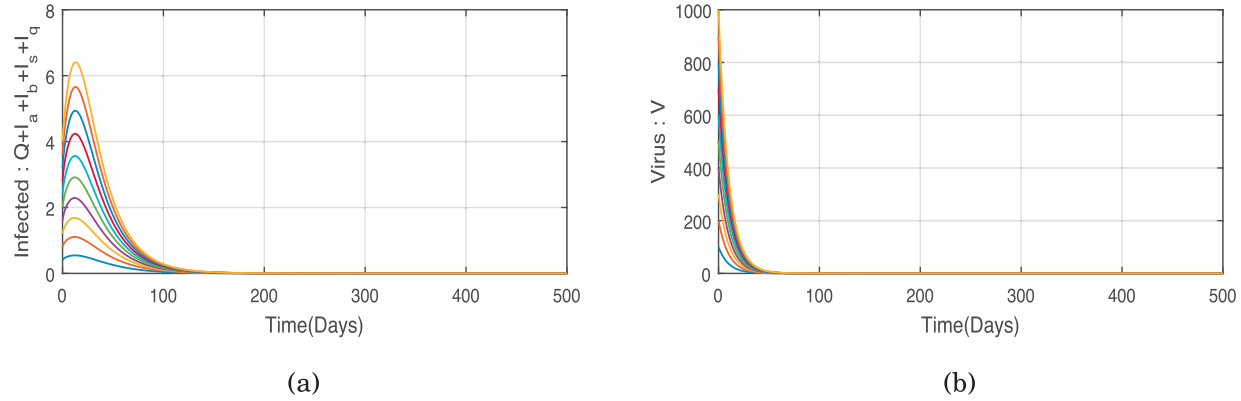

Fig. 2. Simulation of model (4) using various initial conditions when $\Lambda = 10$, $K = 10^6$ and all parameters values are as in Table 1 (so that $\mathcal{R}_0 = 0.69 < 1$). (a) Infected people and (b) Virus density.

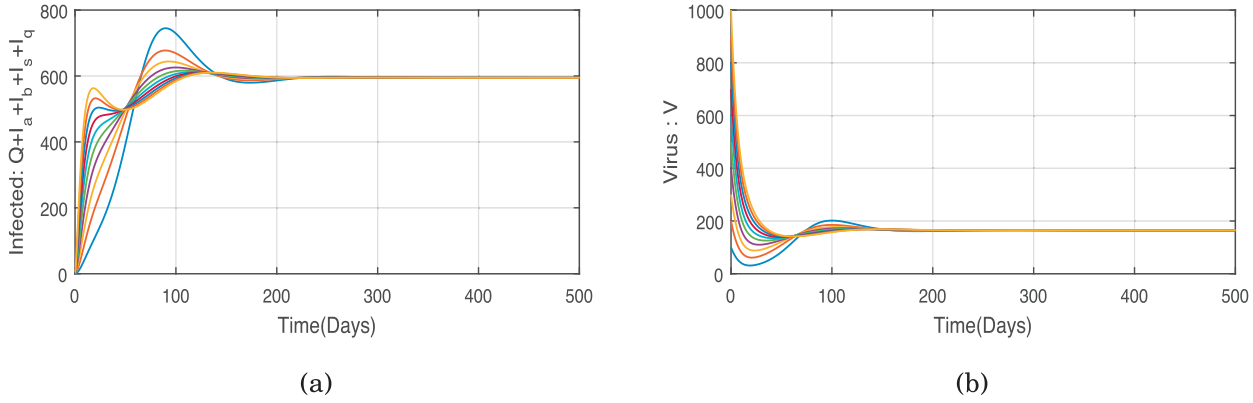

Fig. 3. Simulation of model (4) using various initial conditions when $\Lambda = 100$, $K = 10^3$ and all parameters values are as in Table 1 (so that $\mathcal{R}_0 = 4.01 > 1$). (a) Infected people and (b) Virus density.

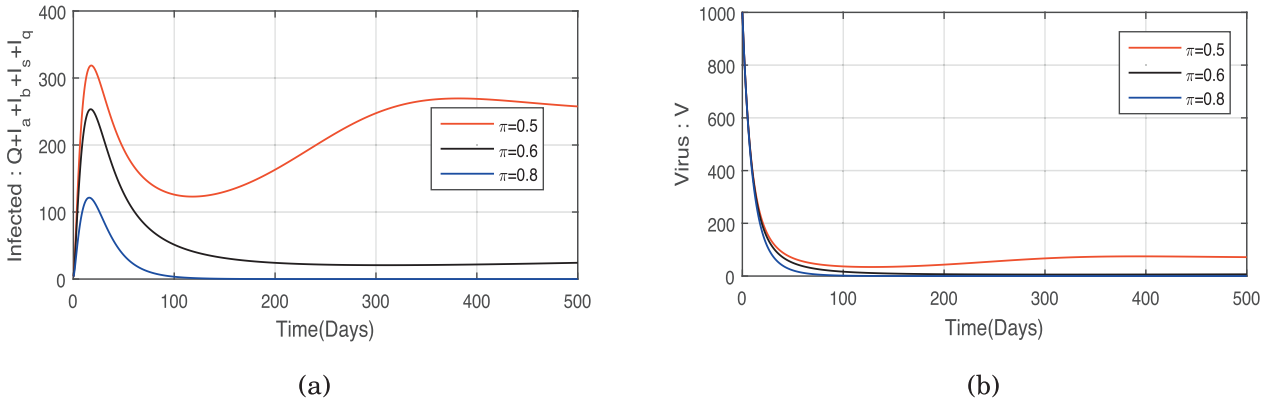

Fig. 4. Simulations of model (4) showing impact of control strategy based on isolation of exposed people (a) Infected people and (b) Virus density.

efforts are made through tracing to isolate 80% of exposed people the disease disappears about 100 days. It is then vital to isolate those who have been exposed to the disease or those coming from affected countries. That's why many countries used contact tracing to identify exposed people to isolate them. Dr Laura Breeher is medical director of occupational health services at the Mayo Clinic (U.S.) and she said: "Contact tracing, it's having a moment of glory right now with *COVID-19* because of the crucial importance of identifying those individuals who have been exposed quickly and isolating or quarantining them" [8].

Confinement: Partial confinement in Cameroon consist to avoid social gathering, imposing travel restrictions and to maintain social distancing [1]. The WHO recommend early execution of this strategies when the disease is detected [9]. The implementation of this control action matches with the increasing of the value of p_2 in our model (4). As we supposed in our model, those who are partially confined have 50% ($\epsilon = 0.5$ in Table 1) less than those that are not confined to be infected. We simulated model (4) for $p_2 = 0.94(\mathcal{R}_0 = 3.03)$, $p_2 = 0.54(\mathcal{R}_0 = 3.08)$ and $p_2 = 0.04(\mathcal{R}_0 = 4.01)$ when $\Lambda = 100$, $K = 10^3$ and all other parameters values are as in Table 1. As we can see in Fig. 5 partial confinement does not have effective impact.

Total confinement reduce strongly movement of population. In that context, every human contacts is strongly pro-

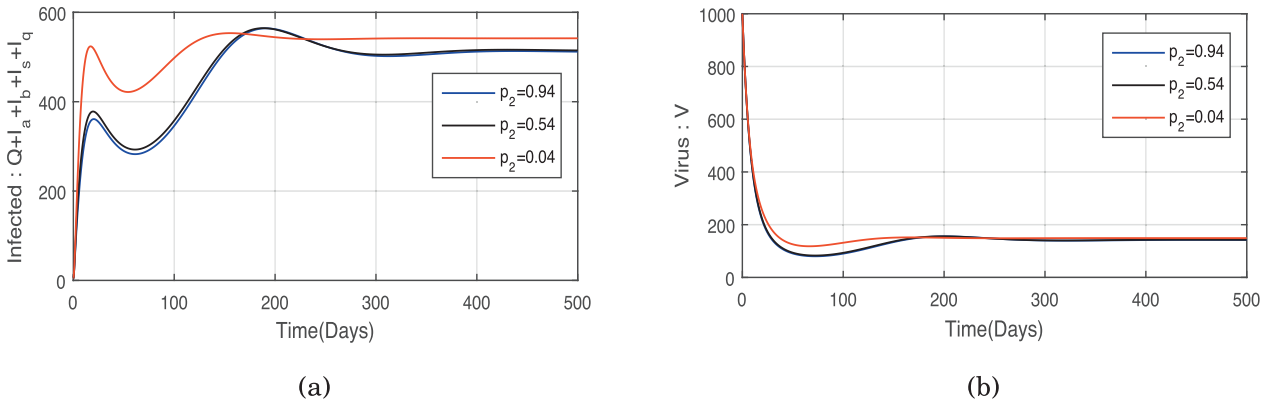

Fig. 5. Simulations of model (4) showing impact of partial confinement of susceptible people (a) Infected people and (b) Virus density.

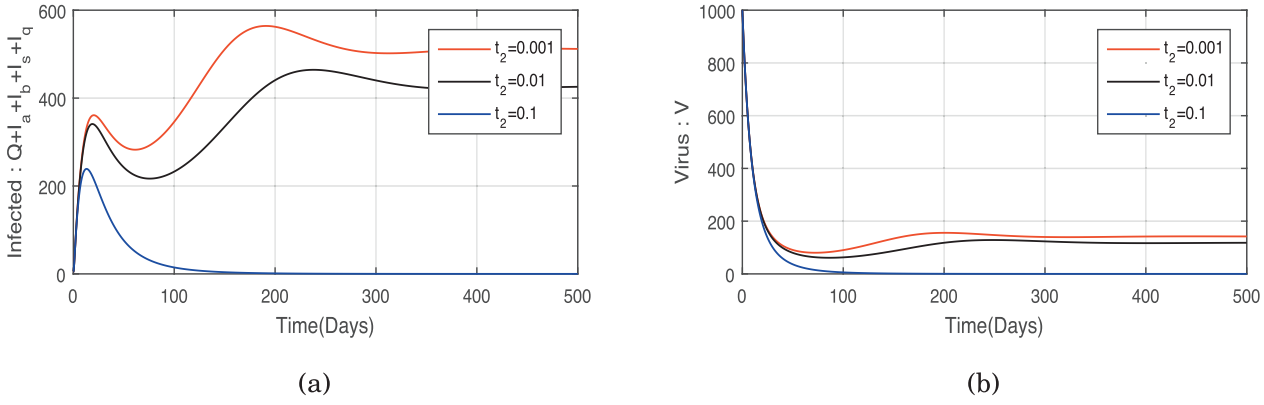

Fig. 6. Simulations of model (4) showing impact of total confinement of susceptible people (a) Infected people and (b) Virus density.

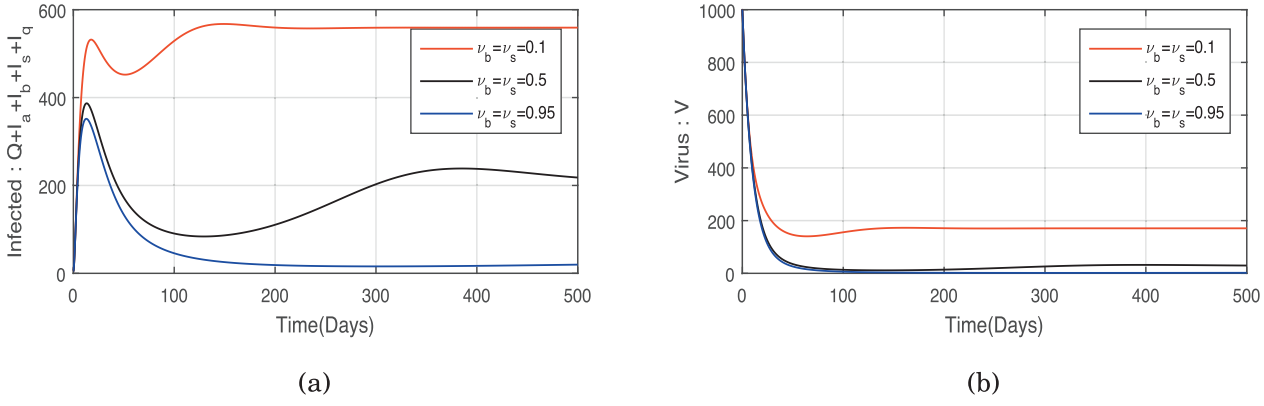

Fig. 7. Simulations of model (4) showing impact of testing (a) Infected people and (b) Virus density.

hibited. So that the value of t_2 increases. But people totally confined are supposed to be partially confined firstly. We simulated model (4) for $t_2 = 0.1(\mathcal{R}_0 = 0.9471)$, $t_2 = 0.01(\mathcal{R}_0 = 2.5)$ and $p_2 = 0.001(\mathcal{R}_0 = 3.03)$ when $\Lambda = 100$, $K = 10^3$, $p_2 = 0.94$ and all other parameters values are as in Table 1. The Fig. 6 illustrate that when at least 10% of those partially confined are totally confined, the disease can disappear after 130 days.

Testing: Testing people for the COVID-19 is important in helping to knowing who has been infected and where can allow the health service to plan, and more effectively cope. Efficient and timely virus testing is a crucial prerequisite for early identification, reporting, isolation, diagnosis, and treatment. Testing casts a direct impact on the effectiveness of epidemic prevention and control. The WHO has called on all countries to ramp up testing programs. Dr Tedros, Director-General of the WHO, made it clear at the media briefing in Geneva on March 16, "We have a simple message for all countries: test, test, test. Test every suspected case." Individuals who have positive tests should be isolated. In Cameroon for example, systematic testing is achieved to those coming at the hospital for medical consultation. This action should increase quickly the value of ν_b and ν_s in model (4). We simulated model (4) for $\nu_b = \nu_s = 0.1(\mathcal{R}_0 = 4.01)$, $\nu_b = \nu_s = 0.5(\mathcal{R}_0 = 1.44)$ and $\nu_b = \nu_s = 0.95(\mathcal{R}_0 = 0.89)$ when $\Lambda = 100$, $K = 10^3$ and all other parameters values are as in Table 1. Fig. 7 illustrates the advantages of testing. If more than 95% of moderate and symptomatic infected people are identified and isolated, the disease is controlled after 100 days.

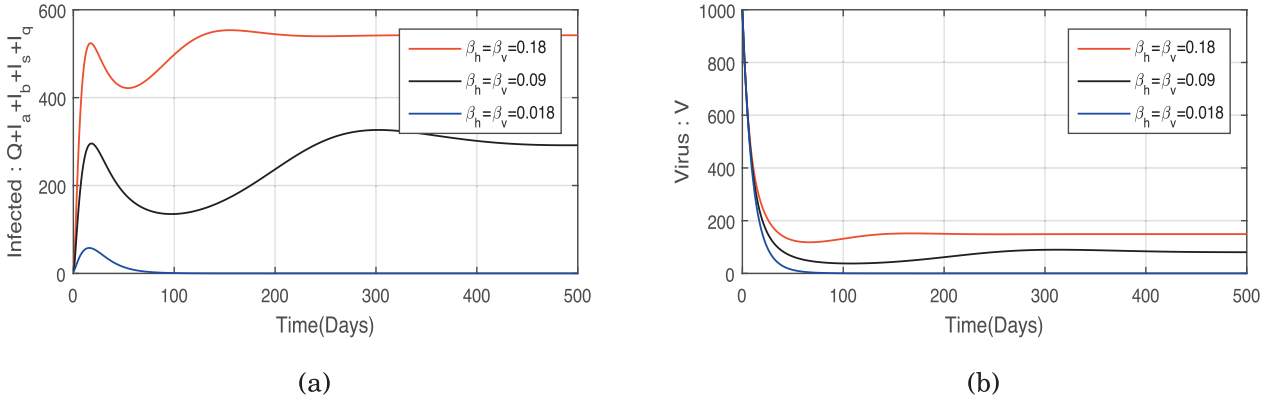

(a) (b)

Fig. 8. Simulations of model (4) showing impact of wearing mask and respect of hygienic rules (a) Infected people and (b) Virus density.

Mask and hygiene rules: Some studies to Hong Kong with hamsters showed that the transmission of *COVID-19* was reduced by more than 60% when the masks are massively used [10]. What should be happened for human population? Otherwise this recommendation is always coupled with the strict respect for hygienic rules. These should really reduce the value of β_h and β_v. We simulated model (4) for $\beta_h = \beta_v = 0.18(\mathcal{R}_0 = 4.01)$, $\beta_h = \beta_v = 0.09(\mathcal{R}_0 = 2.00)$ and $\beta_h = \beta_v = 0.018(\mathcal{R}_0 = 0.40)$ when $\Lambda = 100$, $K = 10^3$ and all other parameters values are as in Table 1. It is obvious to see that reduction for 10% for example of β_h and β_v reduce also 10% values of $\mathcal{R}_0$. Fig. 8 confirm the real impact of these parameters.

5. Conclusion

We presented a mathematical model for the dynamics of *COVID-19* whose first 508 cases were reported in December 2019 in Wuhan-China and the first case was confirmed in Cameroon on March 6, [35]. On June 20, Cameroon reported 10,638 confirmed cases and 282 deaths [54]. In this work, we proposed a *COVID-19* model with the mitigation of control strategies used in Cameroon. The aim was to evaluate the impact of controls strategies based on isolation of exposed people, confinement of human population, testing people living risks area, wearing of masks, and respect of hygienic rules to curtail the spread of *COVID-19* disease. Most of the mathematical models existing in literature are focused on modeling and predicting the disease [45–53,61–63].

We suggest a model that takes into account biological and epidemiological facts known of the disease and the control actions used in Cameroon. A qualitative analysis of the model has been presented. Our findings on the long term dynamics of the system can be summarized as follows: (1) we computed the disease-free equilibrium and derived the basic reproduction number $\mathcal{R}_0$ that determines the outcome of *COVID-19*; (2) we proved that there exists a threshold parameter $\mathcal{R}_c$ such that the disease-free equilibrium is globally asymptotically stable whenever $\mathcal{R}_0 < \mathcal{R}_c < 1$, while when $\mathcal{R}_c < \mathcal{R}_0 < 1$ the model can exhibit the phenomenon of backward bifurcation; (3) the sensitivity analysis of the system has been performed. We found that state variables related to infected people are most sensitive to exposure rates to infected people and the recovery rate of asymptomatic infected people. This suggests that effective control strategies should reduce significantly human contact and to quickly identify asymptomatic infected people in order to isolate and treat them; (4) numerical simulation has been presented to illustrate the theoretical results on the general dynamic of the model. A numerical evaluation of control strategies has been performed. We found that isolation has a real impact on *COVID-19* transmission. When efforts are made through tracing to isolate 80% of exposed people the disease disappears about 100 days. Although partial confinement does not eradicate the disease it is observed that, during partial confinement, when at least 10% of the partially confined population is totally confined, *COVID-19* spread stops after 150 days. The strategy of testing has also a real impact on the disease. In that model, we found that when more than 95% of moderate and symptomatic infected people are identified and isolated, the disease is also really controlled after 90 days. The wearing of mask and respecting hygiene rules are fundamental conditions to control the *COVID-19*. In fact, as we can see in Fig. 8 and by sensitivity analysis, the parameters β_h greatly influence the parameter $\mathcal{R}_0$ more than other parameters. The disease disappear after 75 days when $\beta_h = 0.018$.

The theory and applications of fractional calculus have become extremely useful and important in modeling of biological processes [65] and [66]. Some recent works use fractional calculus compartmental for modeling of infectious disease dynamics [64] and [67]. There are some improvements and extensions of the model (4) on which we are planning to work: the introduction of fractional derivatives and eventually the parameter and state estimation by using available data. We are actually using the fractional derivatives approach in the case of Cholera.

Credit author statement

All authors equally contributed in this manuscript.

Declaration of Competing Interest

The authors declare that they have no known competing financial interests or personal relationships that could have appeared to influence the work reported in this paper.

References

[1] Services du premier ministre. Déclaration spéciale du Premier Ministre, Chef du Gouvernement ce 17 mars2020;https://www.spm.gov.cm.
[2] World statistics. Cameroon. http://www.statistiques-mondiales.com/cameroun.htm.
[3] Jean-Christophe L., Sandrine R., Quitterie R., Nathalie F., Loc B.. Syndrome respiratoire aigu severe coronavirus 2 (*COVID-19*). Hospices Civils Lyons.
[4] Ministry of public health of cameroon. *COVID-19* STATISTICShttp://covid19.minsante.cm/.
[5] Pateron D., Raphal M., Trinh-Duc A.. *COVID-19* Diagnostic et Prise en charge thérapeutique. Elsevier.
[6] Présidence de la république du Cameroun. Coronavirus: mesures instruites par le Président Paul BIYAhttps://www.prc.cm.
[7] Présidence de la république du Cameroun. Reprise des courshttps://www.prc.cm.
[8] TIME. What is contact tracing?Here's How It Could Be Used to Help Fight Coronavirus2020.

[9] World Health Organization (WHO). 2020. https://www.who.int/dg/speeches/detail. WHO Director-General's opening remarks at the media briefing on *COVID*-19, Retrieved 13 March.
[10] France 24, COVID-19 : Hong Kong, l'efficacité des masques est prouvée avec des hamsters. 2020. https://www.france24.com/fr/.
[11] World Health Organization (WHO). https://en.wikipedia.org/wiki/COVID-19_pandemic. Naming the coronavirus disease (*COVID-19*) and the virus that causes it.
[12] Novel coronavirus "China". World Health Organization (WHO)2020;https://www.who.int/csr/don/12-january-2020-novel-coronavirus-china/en/.
[13] Huang C, Wang Y, Li X, Ren L, Zhao J, Hu Y, et al. "Clinical features of patients infected with 2019 novel coronavirus in Wuhan, China". Lancet 2020;395(10223):497–506. doi:10.1016/s0140-6736(20)30183-5. PMC 7159299. PMID 3198626
[14] World Health Organization (WHO). "Statement on the second meeting of the international health regulations (2005) emergency committee regarding the outbreak of novel coronavirus (2019-nCoV)". 2020a. Archived from the original on 31 January 2020. Retrieved 30 January 2020.
[15] World Health Organization (WHO). 2020b. 11 March 2020. Retrieved 11 March 2020. WHO Director-General's opening remarks at the media briefing on *COVID-19*.
[16] ArcGIS. "*COVID-19* Dashboard by the Center for Systems Science and Engineering (CSSE) at Johns Hopkins University (JHU)". Johns Hopkins University; 2020.
[17] World Health Organization (WHO). Q&a on coronaviruses (*COVID-19*). 2020c. Archived from the original on 14 May 2020. Retrieved 14 May.
[18] Centers for Disease Control and Prevention (CDC). How *COVID-19* spreads. 2020a. Archived from the original on 3 April 2020. Retrieved 3 April.
[19] European Centre for Disease Prevention and Control. Q&A on *COVID-19*. 2020.
[20] U.S. Centers for Disease Control and Prevention (CDC), Interim clinical guidance for management of patients with confirmed coronavirus disease (*COVID-19*). 2020b. Retrieved 11 April 2020.
[21] U.S. Centers for Disease Control and Prevention (CDC). Symptoms of novel coronavirus (2019-nCoV). 2020c. Retrieved 11 February 2020.
[22] Velavan TP, Meyer CG. The *COVID-19* epidemic. Tropical Med Int Health 2020;25(3):278–80. doi:10.1111/tmi.13383. PMC 7169770. PMID 32052514
[23] U.S. Centers for Disease Control and Prevention (CDC), Prevention. Caring for yourself at home. 2020d. Retrieved 23 March 2020.
[24] Editorial. The New York Times. Here Comes the Coronavirus Pandemic: Now, after many fire drills, the world may be facing a real fire. 2020. Retrieved 1 March 2020.
[25] IMF Blog. The Great Lockdown: Worst Economic Downturn Since the Great Depression. 2020.
[26] A List of What's Been Canceled Because of the Coronavirus. 2020. Retrieved 11 April 2020. The New York Times.
[27] Scipioni J. Why there will soon be tons of toilet paper, and what food may be scarce, according to supply chain experts. CNBC; 2020.
[28] Watts J, Kommenda N. Coronavirus pandemic leading to huge drop in air pollution. The Guardian; 2020. ISSN 0261–3077
[29] UNESCO. *COVID-19* educational disruption and response. 2020. Retrieved 28 March 2020.
[30] BBC News. Beijing orders 14-day quarantine for all returnees. 2020a. Retrieved 24 March 2020.
[31] Egypt T.. Egypt announces first coronavirus infection. 2020.
[32] BBC News. Nigeria confirms first coronavirus case. 2020b. Retrieved 24 March 2020.
[33] Maclean R. Africa braces for coronavirus, but slowly. The New York Times; 2020.
[34] Burke J, Mumin AA. Somali medics report rapid rise in deaths as *COVID-19* fears grow. The Guardian; 2020.
[35] Kouagheu J. Cameroon confirms first case of coronavirus. Reuters; 2020.
[36] Lukong P, Woussou K. Cameroon, togo report first confirmed cases of coronavirus. Bloomberg; 2020.
[37] Le M.. Au cameroun, sur la piste du coronavirus dans les quartiers de douala. 2020. In French.
[38] TV5MONDE (in French). Coronavirus : le cameroun ferme ses frontires. Retrieved 10 April 2020a.
[39] RFI (in French). Coronavirus: au cameroun, le silence de paul biya, face l'épidémie, fait parler. 2020b.
[40] CRTVweb 9 April 2020. 7 mesures supplémentaires contre la propagation du *COVID-19* au cameroun mesure 1 : port du masque obligatoire. 2020. (Tweet) (in French). Retrieved 10 April 2020 – via Twitter.
[41] JeuneAfrique.com (in French). 2020. Retrieved 18 April 2020. Coronavirus au Cameroun : Paul Biya annonce la libération de certains prisonniers – Jeune Afrique.
[42] Le Monde.fr (in French). 2020. Retrieved 7 May 2020. Au Cameroun, sur la piste du coronavirus dans les quartiers de Douala.
[43] Diekmann O, Heesterbeek JAP, Metz JA. On the definition and the computation of the basic reproduction ratio r0 in models for infectious diseases in heterogeneous populations. J Math Biol 1990;28(4):365–82.
[44] van den Driessche P, Watmough J. Reproduction numbers and the sub-threshold endemic equilibria for compartmental models of disease transmission. J Math Biol 2002;180(4):29–48.
[45] Atangana A. Modelling the spread of COVID-19 with new fractal-fractional operators: can the lockdown save mankind before vaccination? Chaos Solitons Fractals 2020;136:109860.
[46] Kucharski AJ, Russell TW, Diamond C, Liu Y, Edmunds J, Funk S, Eggo RM, Sun F, Jit M, Munday JD, Davies N. Early dynamics of transmission and control of COVID-19: a mathematical modelling study. Lancet Infect Dis 2020;20(5):553–8.
[47] Resmawan R, Yahya L. Sensitivity analysis of mathematical model of coronavirus disease (COVID-19) transmission. CAUCHY 2020;6(2):91–9.
[48] Khan MA, Atangana A. Modeling the dynamics of novel coronavirus (2019-nCoV) with fractional derivative. Alexandria Eng J 2020;59(4):2379–89.
[49] Kassa S., Njagarah H.J., Terefe Y.A.. Analysis of the mitigation strategies for COVID-19: from mathematical modelling perspective. medRxiv; 2020.
[50] Sanchez, Guerrero Y., Sabir Z., Guirao J.L.G.. Design of a nonlinear SITR fractal model based on the dynamics of a novel coronavirus (COVID). 2020.
[51] Nesteruk I.. Estimations of the coronavirus epidemic dynamics in south korea with the use of SIR model. Preprint] ResearchGate 2020.
[52] Liu Z, Magal P, Seydi O, Webb G. Understanding unreported cases in the COVID-19 epidemic outbreak in Wuhan, China, and the importance of major public health interventions. Biology 2020;9(3):50.
[53] Boccaletti S, Ditto W, Mindlin G, Atangana A. Modeling and forecasting of epidemic spreading: the case of COVID-19 and beyond. Chaos Solitons Fractals 2020;135:109794.
[54] Worldometer. https://www.worldometers.info/coronavirus/country/cameroon/. 2020. Retrieved 05 June 2020.
[55] Kamgang JC, Sallet G. Computation of threshold conditions for epidemiological models and global stability of the disease-free equilibrium (DFE). Math Biosci 2008;213:1–12.
[56] Fischer A, Hinrichsen D, Son NK. Stability radii of metzler operators. Vietnam J Math 1998;26(2):147–63.
[57] Narendra KS, Shorten R. Hurwitz stability of Metzler matrices. IEEE Trans Autom Control 2010;55(6):1484–7.
[58] Carr J. Applications of centre manifold theory. Springer Science and Business Media; 2012.
[59] Castillo-Chavez C, Song B. Dynamical models of tuberculosis and their applications. Math Biosci Eng 2004;1(2):361.
[60] Wu J, Dhingra R, Gambhir M, Remais JV. Sensitivity analysis of infectious disease models: methods, advances and their application. J R Soc Interface 2013;10(86):20121018.
[61] Volpert V, Banerjee M, Petrovskii S. On a quarantine model of coronavirus infection and data analysis. Math Model Nat Phenom 2020;15:24.
[62] Bacar N. Un modle mathématique des débuts de lépidémie de coronavirus en france. Math Model Nat Phenom 2020;15 Page 29.
[63] Kochaczyk M, Grabowski F, Lipniacki T. Dynamics of COVID-19 pandemic at constant and time-dependent contact rates. Math Model Nat Phenom 2020;15 Page 28.
[64] Qureshi S, Atangana A. Mathematical analysis of dengue fever outbreak by novel fractional operators with field data. Phys A 2019;526:121127.
[65] Atangana A, Qureshi S. Modeling attractors of chaotic dynamical systems with fractal–fractional operators. Chaos Solitons Fractals 2019;123:320–37.
[66] Atangana A. Application of fractional calculus to epidemiology. In: Cattani C, Srivastava HM, Yang X, De Gruyter O, editors. Fractional dynamic; 2015. p. 174–90.
[67] Aliyu AI, Inc M, Yusuf A, Baleanu D. A fractional model of vertical transmission and cure of vector-borne diseases pertaining to the Atangana Baleanu fractional derivatives. Chaos Solitons Fractals 2018;116(1):268–77.